animals

MDPI

Article

Ghrelin Accelerates Nuclear Maturation of Bovine Oocytes and Is Associated with PI3K-Akt Signaling and Redox Homeostasis

Ruizhen Jian [1,2,3,4,†], Chuanqiang Zhang [1,4,†], Kuo Li [5], Xingyu Zhang [1,2,3], Daqing Wang [1,2,3], Zeyu Lu [4], Yanyan Yang [4], Lanting Wang [1,2,3], Xiaoxuan Fan [1,2,3], Yong Zhang [1,2,3,*] and Guifang Cao [1,2,3,6,*]

[1] College of Veterinary Medicine, Inner Mongolia Agricultural University, Hohhot 010011, China; jianruizhen0503@163.com (R.J.); zhangcq313@163.com (C.Z.); 17725760839@163.com (X.Z.); 18947567494@163.com (L.W.); 18804933631@163.com (X.F.)
[2] Animal Embryo and Developmental Engineering Key Laboratory of Higher Education, Institutions of Inner Mongolia Autonomous Region, Hohhot 010011, China
[3] Inner Mongolia Autonomous Region Key Laboratory of Basic Veterinary Medicine, Hohhot 010011, China
[4] Inner Mongolia Academy of Agricultural and Animal Husbandry Sciences, Hohhot 010031, China; 15248157808@163.com (Z.L.); swallow_0088@163.com (Y.Y.)
[5] College of Veterinary Medicine, Northwest A&F University, Yangling 712100, China; lkuo777@163.com
[6] College of Life Sciences, Inner Mongolia University, Hohhot 010021, China
* Correspondence: zhy1956@263.net (Y.Z.); guifangcao@126.com (G.C.); Tel.: +86-13848120488 (G.C.)
† These authors contributed equally to this work.

Simple Summary

In vitro embryo production in cattle is limited by incomplete oocyte maturation. Ghrelin is a metabolic peptide involved in reproductive regulation; however, its effects on bovine oocyte maturation remain unclear, as previous studies have reported inconsistent findings. This study investigated the effects of exogenous ghrelin supplementation and the underlying mechanisms during in vitro maturation (IVM) of bovine cumulus-oocyte complexes (COCs). Ghrelin-like immunoreactive signals were observed in COCs and oocytes, whereas ghrelin mRNA exhibited dynamic expression during IVM. Supplementation with 50 ng/mL exogenous ghrelin accelerates nuclear maturation and increases the rate of first polar body extrusion after 16 h of IVM, accompanied by the upregulation of *HAS2*, *GDF9*, and *BMP15*. Transcriptomic analysis and pharmacological inhibition suggested that these effects were associated, at least in part, with the phosphatidylinositol 3-kinase/protein kinase B (PI3K-Akt) signaling pathway. In addition, ghrelin was associated with increased intracellular glutathione (GSH) levels, decreased reactive oxygen species (ROS) accumulation, and altered mitochondrial and lysosomal fluorescence signals. These findings suggest that ghrelin accelerates bovine oocyte nuclear maturation and is accompanied by transcriptional changes consistent with PI3K-Akt signaling and by an altered GSH redox status. However, whether this acceleration translates into improved oocyte quality or developmental competence remains to be determined.

Abstract

Ghrelin is a metabolic and reproductive peptide that may influence oocyte competence, but its role in bovine oocyte in vitro maturation (IVM) remains insufficiently defined. This study investigated the effects of exogenous ghrelin supplementation on bovine oocyte nuclear maturation and examined its potential association with PI3K-Akt signaling and intracellular redox status. Bovine cumulus-oocyte complexes (COCs) were cultured with 50 ng/mL ghrelin, and maturation was evaluated based on the rate of first polar body extrusion and the expression of maturation-related genes. Ghrelin-like immunoreactivity and temporal transcript abundance were examined in cumulus cells and oocytes. RNA sequencing was performed using a 2 × 2 design comprising ghrelin treatment and IVM duration as the

Check for updates

Academic Editor: Maria De Falco

Received: 22 October 2026
Revised: 11 November 2026
Accepted: 18 November 2026
Published: 24 November 2026

Copyright: © 2026 by the authors. Licensee MDPI, Basel, Switzerland. This article is an open access article distributed under the terms and conditions of the Creative Commons Attribution (CC BY) license.

two factors. Differentially expressed genes were subjected to pathway enrichment analysis, followed by pharmacological intervention with the PI3K-Akt inhibitor LY294002 to further assess the involvement of PI3K-Akt signaling. Intracellular glutathione (GSH) and reactive oxygen species (ROS) fluorescence, mitochondrial and lysosomal fluorescence signals, and mitochondrial membrane potential were also evaluated. Ghrelin immunoreactivity was detected in immature COCs and denuded oocytes, while the relative abundance of ghrelin transcripts exhibited a time-dependent pattern during IVM. Ghrelin treatment increased the rate of first polar body extrusion at 16 h and enhanced the expression of *HAS2*, *GDF9*, and *BMP15*. Pathway enrichment analysis revealed that differentially expressed genes associated with ghrelin treatment and IVM duration were enriched in GSH metabolism and the PI3K-Akt signaling pathway. LY294002 altered ghrelin-associated expression patterns of *VEGFA*, *FGF2*, *BCL-2*, and *BAX*. Ghrelin-treated oocytes also showed increased GSH fluorescence, reduced ROS fluorescence, altered mitochondrial and lysosome-related fluorescence signals, and a higher JC-1 red-to-green fluorescence ratio. These findings suggest that ghrelin accelerates bovine oocyte nuclear maturation at 16 h of IVM and is accompanied by transcriptional changes consistent with PI3K-Akt signaling and by an altered GSH redox status, without establishing direct pathway activation.

Keywords: bovine oocyte; ghrelin; in vitro maturation; nuclear maturation; PI3K-Akt signaling; glutathione; reactive oxygen species; mitochondrial membrane potential

1. Introduction

In vitro maturation (IVM) of oocytes is a fundamental component of assisted reproductive technologies and is widely applied in bovine in vitro embryo production, including in vitro fertilization, somatic cell nuclear transfer, and the dissemination of superior livestock genetics [1,2]. The acquisition of oocyte developmental competence requires not only the completion of nuclear maturation, typically assessed by the rate of first polar body extrusion, but also adequate cytoplasmic maturation. Cytoplasmic maturation involves coordinated molecular and metabolic events, including RNA and protein storage, mitochondrial redistribution, energy production, antioxidant defense, and bidirectional communication between the oocyte and surrounding cumulus cells [2–4]. Despite substantial advances in bovine IVM systems, oocytes matured under in vitro conditions generally have lower developmental competence than their in vivo-matured counterparts. One likely explanation is that conventional culture systems do not fully mimic the changing follicular microenvironment, where metabolic substrates, antioxidant protection, and endocrine and paracrine cues jointly support Cumulus–oocyte complex (COCs) function [1,3,4].

Oxidative stress is widely recognized as an important contributor to the loss of oocyte quality during IVM. Reactive oxygen species (ROS) are not exclusively detrimental; at physiological levels, they function in intracellular signaling and help regulate meiotic events. Problems arise when ROS accumulate beyond the cellular antioxidant capacity, disturbing redox equilibrium and damaging lipids, proteins, DNA, and organelles [5,6]. In bovine oocytes, oxidative stress has been linked to defective spindle assembly, mitochondrial impairment, a decline in mitochondrial membrane potential, insufficient ATP production, apoptosis-associated changes, and poorer subsequent embryonic development [5–8]. Glutathione (GSH), the predominant non-enzymatic antioxidant in mammalian oocytes, plays a central role in intracellular redox homeostasis [9]. Greater GSH availability during IVM can facilitate ROS removal, help maintain mitochondrial function, and support cytoplasmic maturation; it is also positively related to subsequent fertilization and embryo development [10]. Accordingly, the addition of bioactive compounds capable of strengthening

antioxidant defenses and maintaining organelle homeostasis has become a frequently considered approach to improving bovine oocyte competence in vitro. However, the molecular mechanisms by which these compounds jointly influence redox status, cell survival, and meiotic progression have not yet been fully defined.

Ghrelin is a 28-amino-acid acylated peptide originally identified as the endogenous ligand for the growth hormone secretagogue receptor (GHSR) [11]. In addition to its established roles in growth hormone release, appetite regulation, and energy metabolism, ghrelin is increasingly recognized as a regulator of reproductive function [12]. Ghrelin and/or GHSR expression has been reported in reproductive tissues, including the ovary, where ghrelin may influence follicular development, steroidogenesis, granulosa-cell function, and local energy metabolism [12,13], moreover, ghrelin has been shown in different cellular systems to exert antioxidant and anti-apoptotic effects [14–16]. Phosphatidylinositol 3-kinase/protein kinase B (PI3K-Akt) is a central signaling cascade involved in the regulation of cell survival, metabolism, oxidative stress responses, and apoptosis [15,16]. In the ovary, this pathway has an established role in follicle activation and oocyte development [17,18]. However, the role of ghrelin in bovine oocyte IVM, particularly its relationship with PI3K-Akt survival signaling and GSH-mediated redox regulation, remains unclear.

In our previous study, a concentration-gradient screening experiment identified 50 ng/mL ghrelin as the optimal concentration for promoting bovine oocyte maturation [19]. At this concentration, ghrelin increased the proportion of oocytes undergoing first polar body extrusion and shortened the IVM period required to achieve maturation from 24 h to 16 h. However, the molecular mechanisms underlying the maturation-promoting effect of ghrelin remain poorly understood. Therefore, based on our previous findings, 50 ng/mL exogenous ghrelin was used in all subsequent functional experiments in the present study. We investigated ghrelin-like immunoreactivity in immature COCs and oocytes, characterized the temporal expression pattern of ghrelin during IVM, and evaluated the effects of ghrelin on oocyte nuclear maturation and maturation-related gene expression. Transcriptome sequencing was subsequently performed to identify ghrelin-associated differentially expressed genes and enriched pathways. KEGG pathway enrichment analysis of upregulated differentially expressed genes revealed two significantly enriched pathways: the PI3K-Akt signaling pathway, which exhibited the highest GeneRatio and the largest number of enriched genes, and the GSH metabolism pathway, which was the most significantly enriched metabolic pathway. The PI3K-Akt pathway is a key regulator of meiotic resumption, oocyte survival, and mitochondrial function. It has also been implicated in cellular responses to oxidative stress, the regulation of apoptosis, and DNA damage repair. In several mammalian models, persistent activation of PI3K-Akt signaling has been reported to increase the expression of factors associated with oocyte maturation, limit apoptotic signaling, and improve indices of cytoplasmic quality. GSH metabolism represents another important endogenous defense mechanism in oocytes. As the major non-enzymatic antioxidant system, it contributes to the removal of excess ROS and helps maintain intracellular redox balance during in vitro culture.

Because these pathways may be involved in distinct but potentially interconnected aspects of oocyte maturation, we hypothesized that ghrelin may promote bovine oocyte IVM through two related processes. First, ghrelin may be associated with PI3K-Akt signaling, potentially influencing apoptosis-related gene expression and nuclear maturation. Second, it may be involved in GSH-associated redox homeostasis and thereby reduce oxidative stress. To examine this hypothesis, PI3K-Akt signaling was pharmacologically inhibited with LY294002. GSH and ROS fluorescence signals were measured using fluorescence-based methods to evaluate intracellular redox status. We combined endogenous expression profiling, exogenous ghrelin treatment, transcriptomic analysis, pathway inhibition, and

validation of organelle function to investigate the association of ghrelin with bovine oocyte maturation in vitro. These experiments provide insight into the molecular processes associated with ghrelin action and may inform the optimization of bovine oocyte culture systems for large-scale embryo production.

2. Materials and Methods

2.1. Reagents and Instruments

Unless otherwise stated, all reagents were of analytical grade and obtained from commercial suppliers. Ghrelin was purchased from Peptides International (Cat. No. PGH-3625-PI, Louisville, KY, USA). OPU medium (Cat. No. REF2.01.500) and IVM medium (Cat. No. REF1.03.020) were obtained from MediCult/Stroebech Medi (Hundested, Denmark). The commercial IVM medium used in this study contains FSH, LH, and EGF according to the manufacturer's instructions. Ghrelin was supplemented additionally on top of this standard maturation system. Hyaluronidase (Cat. No. H4272), dimethyl sulfoxide (DMSO; Cat. No. D2650), and other routine reagents were purchased from Sigma-Aldrich (St. Louis, MO, USA). Medium 199 (Cat. No. 11150059), Dulbecco's phosphate-buffered saline (DPBS; Cat. No. C3590-0500), and other cell-culture reagents were obtained from Gibco (Waltham, MA, USA). LY294002, a PI3K-Akt inhibitor, was purchased from MedChemExpress (Cat. No. HY-10108, Monmouth Junction, NJ, USA). Rabbit anti-human ghrelin primary antibody (Cat. No. bs-0467R), Alexa Fluor 488-conjugated goat anti-rabbit IgG (H + L) secondary antibody (Cat. No. bs-0295G-AF488), and normal goat serum (Cat. No. C-0005) were obtained from Bioss Antibodies (Beijing, China). Paraformaldehyde (4%; Cat. No. P1110) was purchased from Solarbio Science & Technology Co., Ltd. (Beijing, China). Fluorescence probes and assay kits included a reactive oxygen species (ROS) detection kit (Cat. No. S0035S), JC-1 mitochondrial membrane-potential assay kit (Cat. No. C2003S), LysoTracker Red (Cat. No. C1046), MitoTracker Red CMXRos (Cat. No. C1035), and DAPI Staining Solution (Cat. No. C1006), all obtained from Beyotime Biotechnology (Shanghai, China). CellTracker Blue CMF2HC dye (Cat. No. 215868-45-4) was purchased from MedChemExpress (Monmouth Junction, NJ, USA). TransScript Uni Cell to cDNA Synthesis SuperMix for qPCR (Cat. No. AC301-01) was obtained from TransGen Biotech (Beijing, China). An electrophoresis system (Bio-Rad Laboratories, Hercules, CA, USA), a CO_2 incubator (Thermo Fisher Scientific, Waltham, MA, USA), benchtop and refrigerated centrifuges, a fluorescence microscope (Olympus Corporation, Tokyo, Japan), and a laser-scanning confocal microscope (LSM 880; Carl Zeiss AG, Oberkochen, Germany) were used in this study.

2.2. Oocyte Collection and IVM

In the present study, bovine oocytes were obtained using ovum pick-up (OPU) rather than from ovaries collected at a local slaughterhouse. This approach was selected because OPU allows oocytes to be recovered from live donor cattle under a controlled and standardized collection schedule, thereby minimizing the effects of postmortem deterioration, prolonged transport, and uncontrolled variation in follicular and ovarian status. In addition, OPU-derived oocytes are more representative of oocytes obtained from reproductively active donor animals and are therefore suitable for evaluating the effects of in vitro culture conditions on oocyte maturation and subsequent molecular responses.

Oocytes were collected by OPU from Holstein cattle at a cattle farm in Hohhot, China. The cows were cycling, clinically healthy, non-pregnant, and had normal ovarian function. Follicles measuring approximately 3–8 mm in diameter were aspirated using an OPU system equipped with an 18-gauge disposable OPU needle. The aspirated follicular fluid and ovarian contents were collected in collection cups and transported to the laboratory within 2 h.

COCs were then selected under a stereomicroscope according to previously established morphological criteria [1,3]. Only COCs containing a morphologically homogeneous oocyte with a uniform cytoplasm and at least three compact layers of surrounding cumulus cells were used. Selected COCs were washed three times in pre-equilibrated OPU medium, twice in H-M199 washing medium, and twice in IVM medium. Unless otherwise stated, approximately 50 COCs were cultured in 500 μL of IVM medium per well in four-well culture plates. The plates were incubated at 38.5 °C in a humidified atmosphere containing 5% CO_2 for the indicated maturation periods. The four-group nuclear maturation experiment was conducted across three separately performed collection-and-culture batches, each constituting one biological replicate. Within each batch, eligible COCs were pooled and randomly allocated to four experimental groups, with 50 COCs per group and 200 COCs per batch. A total of 600 COCs were allocated across the three biological replicates, corresponding to 150 COCs per group. First polar body extrusion rates were calculated separately for each group within each batch, and these batch-level proportions were used for statistical analysis, with $n = 3$ biological replicates.

2.3. Immunofluorescence Localization of Ghrelin

The cellular localization of ghrelin was examined in intact COCs and denuded oocytes. Samples were washed three times in DPBS containing 0.1% bovine serum albumin (BSA) and fixed in 4% paraformaldehyde at 4 °C for 24 h. To obtain denuded oocytes, COCs were incubated in 0.1% hyaluronidase at room temperature for 3 min and gently pipetted until the cumulus cells were removed. Fixed samples were permeabilized with 1% Triton X-100 for 20 min and blocked with 5% normal goat serum for 20 min at room temperature. The samples were then incubated overnight at 4 °C with rabbit anti-human ghrelin primary antibody diluted in blocking solution at 1:100. Primary-antibody-omission control samples were processed in parallel with the experimental samples. In these controls, the primary antibody was replaced with blocking solution. The secondary-antibody incubation, DAPI counterstaining, washing, mounting, and imaging steps were otherwise identical to those used for the primary-antibody-incubated samples. After three washes in DPBS containing 0.1% BSA, the samples were incubated with Alexa Fluor 488-conjugated goat anti-rabbit IgG (H + L) secondary antibody at 1:200 for 1 h at 37 °C in the dark. Nuclei were counterstained with DAPI for 5–10 min. Samples were washed at least three times, with each wash lasting 5 min, mounted using an anti-fade mounting medium, and examined using a laser-scanning confocal microscope. Images were acquired using identical laser power, detector gain, offset, pinhole, and magnification settings within each experiment.

2.4. Temporal Expression Analysis of Ghrelin in Cumulus Cells and Oocytes

To characterize the temporal expression pattern of ghrelin during IVM, COCs were collected at 0, 6, 12, 18, and 24 h of culture. COCs were incubated in 0.1% hyaluronidase at 37 °C for 3 min and gently pipetted in M199 to remove the cumulus cells. The denuded oocytes were collected separately, whereas the cumulus-cell suspension was transferred to sterile tubes and centrifuged at 1500 rpm for 5 min. The supernatant was discarded, and the cell pellets were washed once in DPBS before RNA isolation. Because bovine oocytes contain limited amounts of RNA, samples were processed using a single-cell-compatible lysis and reverse-transcription system. Cell lysates were prepared using C-to-C Lysis Buffer. For cultured cells, the culture medium was discarded, and the cells were washed with pre-chilled PBS, which was then completely aspirated. A total volume of 40 μL C-to-C Lysis Buffer was added, and the samples were incubated at room temperature for 5 min, followed by incubation at 75 °C for 5 min. Samples were immediately placed on ice, and the resulting lysates were directly used for reverse-transcription reaction. Cell lysates were prepared by

mixing 15 μL of cell-lysis solution with 1 μL of TransScript cDNA synthesis enzyme mix and 4 μL of 5× TransScript cDNA synthesis buffer. The mixture was incubated at 50 °C for 5 min, followed by enzyme inactivation at 85 °C for 2 min. The resulting cDNA was stored at −80 °C until qRT-PCR analysis. The expression of ghrelin was quantified relative to *GAPDH* using the $2^{-\Delta\Delta Ct}$ method. Each biological replicate consisted of 50 oocytes or cumulus-cell preparations, and 3 independent biological replicates were analyzed.

2.5. Effects of Ghrelin on Oocyte Maturation Kinetics

To evaluate the effect of ghrelin on the kinetics of bovine oocyte maturation, COCs were randomly assigned to a control group or a ghrelin-treatment group. The ghrelin group was cultured in IVM medium supplemented with 50 ng/mL ghrelin (G50), whereas the control group was cultured in IVM medium supplemented with an equivalent volume of the ghrelin vehicle. Samples were collected after 16 or 24 h of IVM. Following removal of cumulus cells with 0.1% hyaluronidase, nuclear maturation was assessed by determining the first polar body extrusion rate under a stereomicroscope. The first polar body extrusion rate was calculated as the number of oocytes with an extruded first polar body divided by the total number of morphologically intact oocytes examined, multiplied by 100. Cumulus cells and denuded oocytes were collected separately for gene-expression analysis. The expression of the cumulus expansion-related gene *HAS2* was examined in cumulus cells, whereas the oocyte-secreted factor genes *GDF9* and *BMP15* were analyzed in denuded oocytes. Based on the combined evaluation of first polar body extrusion and maturation-related gene expression, the optimal sampling time for the G50 group was selected for subsequent transcriptomic, inhibitor-intervention, and fluorescence-based analyses. The number of COCs analyzed in each group was 50, with three independent biological replicates.

2.6. RNA Sequencing and Bioinformatic Analysis

For transcriptome analysis, MII-stage oocytes were collected from four experimental groups generated by a 2 × 2 factorial design comprising ghrelin treatment and culture duration: control oocytes cultured for 16 h (CON-16 h), ghrelin-treated oocytes cultured for 16 h (G50-16 h), control oocytes cultured for 24 h (CON-24 h), and ghrelin-treated oocytes cultured for 24 h (G50-24 h). Three independent biological replicates were prepared for each group, with 50 oocytes per replicate.

To characterize the effects of ghrelin treatment, culture duration, and their interaction, differential expression analysis was performed using the DESeq2 R package (v1.20.0) [20]. The factorial model included batch, ghrelin treatment, culture time, and the ghrelin-by-time interaction, specified as ~ batch + ghrelin * time. This model was used to estimate the main effect of ghrelin, the main effect of culture duration, and the ghrelin-by-time interaction effect. Pathway-level enrichment analysis was subsequently performed for genes associated with each significant effect.

In addition to the factorial analysis, three biologically motivated pairwise comparisons were performed. First, the isochronic treatment comparison between G50-16 h and CON-16 h was used to characterize transcriptional changes associated with ghrelin at the same culture duration. Second, the time-course reference comparison between CON-24 h and CON-16 h was used to characterize transcriptional changes associated with normal maturation progression in untreated oocytes. Third, the phenotype-based exploratory comparison between G50-16 h and CON-24 h was performed because these two groups had been shown in the preceding experiments to exhibit comparable maturation phenotypes. This comparison was used to identify transcriptional features associated with the matched maturation phenotype. Because the comparison differed in both ghrelin treatment and

culture duration, the resulting transcriptional differences were not interpreted as ghrelin-specific effects independent of culture duration.

Total RNA was extracted from pooled oocyte lysates (50 oocytes per biological replicate). Libraries were constructed using the NEBNext Ultra RNA Library Prep Kit for Illumina (New England Biolabs, Ipswich, MA, USA) according to the manufacturer's instructions, involving poly(A) mRNA enrichment, fragmentation, first- and second-strand cDNA synthesis, end repair, adapter ligation, and PCR amplification. Paired-end sequencing (PE150) was performed on the Illumina NovaSeq platform by Novogene Co., Ltd. (Beijing, China). Raw reads were processed to remove adapter-containing reads, reads with excessive proportions of undetermined bases (N), and low-quality reads. The resulting clean reads were used for downstream analyses. Clean reads were aligned to the bovine reference genome (Bos taurus ARS-UCD1.2) using HISAT2 (v2.0.5) [21]. Gene-level read counts were generated using feature Counts (v1.5.0-p3). Principal-component analysis and sample-correlation analysis were performed to evaluate replicate consistency, group separation, and potential batch effects. Genes with an absolute log2 fold change greater than 1 and an adjusted *p*-value, calculated using the Benjamini–Hochberg false discovery rate (FDR), of less than 0.05 were considered differentially expressed genes (DEGs). Gene Ontology (GO) functional enrichment and Kyoto Encyclopedia of Genes and Genomes (KEGG) pathway enrichment analyses were performed using the clusterProfiler R package (v3.8.1). GO terms and KEGG pathways with an adjusted *p*-value of less than 0.05 were considered significantly enriched. The factorial analysis was used as the primary framework for separating treatment, time, and interaction effects, whereas the three pairwise comparisons were used to describe the corresponding biological patterns and the accelerated-maturation phenotype.

2.7. PI3K-Akt Inhibitor Treatment and Experimental Groups

DEGs identified in the phenotype-based exploratory comparison between G50-16 h and CON-24 h were significantly enriched in the PI3K-Akt signaling pathway and the GSH metabolism pathway. Because these two groups had been shown in the preceding experiments to exhibit comparable maturation phenotypes, these enriched pathways were considered candidate molecular pathways associated with the matched maturation phenotype. Because the PI3K-Akt signaling pathway was selected for functional assessment, LY294002 was used as a pharmacological PI3K-Akt inhibitor to investigate its potential contribution to the ghrelin-associated accelerated-maturation response.

LY294002 was dissolved in Dimethyl sulfoxide (DMSO) to prepare a 10 mM stock solution and stored at −80 °C. The final DMSO concentration was kept identical in all experimental groups, including the vehicle control. To determine the working concentration of LY294002, COCs were cultured for 24 h in IVM medium containing 0, 5, 10, 15, and 20 μM LY294002. The first polar body extrusion rate and the mRNA levels of oocyte maturation-related genes was then determined. Each concentration was tested in three independent biological replicates. Because 20 μM LY294002 significantly reduced first polar body extrusion and would therefore confound pathway inhibition with suppressed nuclear maturation, 10 μM was selected: at this concentration *HAS2* and *GDF9* expression was significantly decreased without a significant change in first polar body extrusion.

For pathway-intervention experiments, COCs were randomly allocated to four groups: the CON group, cultured in IVM medium containing the equivalent volume of DMSO; the G50 group, cultured in IVM medium containing 50 ng/mL ghrelin; the LY294002 group, cultured in IVM medium containing 10 μM LY294002; and the LY294002 + G50 group, pretreated with 10 μM LY294002 for 30 min and subsequently cultured with 50 ng/mL ghrelin in the continued presence of LY294002. All groups were cultured for 16 h. After

maturation, cumulus cells were removed, and denuded oocytes were collected for RNA extraction and qRT-PCR analysis. The expression of *VEGFA* and *FGF2* was evaluated as candidate pathway-associated genes, whereas *BAX* and *BCL-2* were analyzed as apoptosis-related genes. The primer sequences are provided in Supplementary Table S1.

2.8. Quantitative Real-Time PCR

Cell lysates were processed using the TransScript Uni Cell to cDNA Synthesis SuperMix for qPCR according to the manufacturer's instructions. qRT-PCR was performed using Bio-Rad in a final reaction volume of 20 μL containing 2 μL of cDNA template, 0.4 μL of each forward and reverse primer, 10 μL of qPCR master mix, and 7.2 μL of nuclease-free water. The amplification protocol was as follows: initial denaturation at 95 °C for 3 min; 40 cycles of denaturation at 95 °C for 15 s, annealing at 60 °C for 30 s, and extension at 72 °C for 30 s; followed by a final extension at 72 °C for 5 min. Amplification specificity was assessed by melting-curve analysis, with a no-template control included in every assay. Before GAPDH was selected as the reference gene, its expression stability was examined across the experimental groups. Target-gene expression was normalized to *GAPDH* and quantified using the $2^{-\Delta\Delta Ct}$ method. The primer sequences, amplicon lengths, and amplification efficiencies are provided in Supplementary Table S1. Three independent biological replicates were analyzed, with each sample assessed in triplicate.

2.9. Assessment of Intracellular Gsh, Ros, Mitochondria, Lysosomes, and Mitochondrial Membrane Potential

To determine whether the transcriptome-associated changes were accompanied by corresponding cellular phenotypes, intracellular GSH levels, ROS accumulation, mitochondrial activity, lysosomal status, and mitochondrial membrane potential were further examined in mature oocytes from the G50-16 h and CON-24 h groups. Approximately 50 oocytes from each group were examined in each of three independent biological replicates. All staining procedures were repeated independently three times. Before staining, the oocytes were washed with sterile DPBS, and subsequent staining and handling were carried out under reduced-light conditions. Intracellular GSH was detected with CellTracker Blue CMF2HC. Oocytes were incubated with 5 μM CellTracker Blue CMF2HC at 37 °C for 25 min, washed three times with DPBS, and examined using a laser-scanning confocal microscope. Intracellular ROS were assessed with CM-H_2DCFDA. Following incubation at 37 °C for 25 min, the oocytes were washed three times and imaged using the appropriate excitation and emission settings. Lysosomal fluorescence was evaluated with LysoTracker Red. For this assay, the oocytes were incubated with 200 nM LysoTracker Red at 37 °C for 60 min, washed three times with DPBS, and imaged by confocal microscopy. Mitochondrial fluorescence was assessed with MitoTracker Red CMXRos. Oocytes were incubated with the working solution at 37 °C for 30 min, washed three times, and imaged using identical acquisition settings within each biological replicate.

MMP was measured using JC-1. Freshly prepared JC-1 working solution was added to mature oocytes, which were then incubated at 37 °C for 25 min in the dark. The oocytes were washed three times with DPBS to remove unbound probe and immediately imaged. JC-1 monomers produce green fluorescence, whereas JC-1 aggregates produce red fluorescence. Excitation and emission settings were selected in accordance with the manufacturer's instructions and the configuration of the microscope. Red and green fluorescence images were acquired for each oocyte under identical acquisition parameters, and MMP was expressed as the red-to-green fluorescence ratio [22]. Images were analyzed with ImageJ version 1.8.0 (National Institutes of Health, Bethesda, MD, USA). Fluorescence intensity was measured after background subtraction. The region of interest encompassed the oocyte

and excluded surrounding debris. Changes in mitochondrial and lysosomal fluorescence were interpreted as alterations in signal intensity or distribution; these measurements were not taken as direct estimates of organelle number or functional activity.

Fixed oocytes were incubated with DAPI staining solution at room temperature in the dark for 3–5 min. After the staining solution was aspirated, the oocytes were washed 2–3 times with PBS-PVA for 3–5 min each. The oocytes were then mounted onto glass slides and observed under a confocal laser scanning microscope. Oocytes that had extruded the first polar body and in which a normal MII chromosome metaphase plate and polar body chromatin were observed by DAPI staining were classified as MII-stage oocytes.

2.10. Statistical Analysis

Fluorescence images were analyzed with ImageJ version 1.8.0. Each experiment was performed with three independent biological replicates unless otherwise stated. Technical replicates, when included, were averaged within each biological replicate and were not treated as independent statistical units. Statistical analyses were carried out in GraphPad Prism version 7.0 (GraphPad Software, San Diego, CA, USA).

All proportional data, including the first polar body extrusion rate and the proportion of PB-extruded oocytes reaching the MII stage, were considered non-normally distributed and were analyzed exclusively using nonparametric tests.the percentage of each biological replicate was defined as the statistical unit ($n = 3$); individual oocytes were treated only as observational units. Normality and homogeneity of variance were assessed prior to analysis. Suitable parametric or nonparametric tests were selected according to the distribution characteristics and experimental design, and detailed information for each dataset is provided in the corresponding figure legends. For fluorescence-related indicators, statistical tests were selected based on experimental design and are described in the relevant figure legends. For gene expression data, normality and homogeneity of variance were assessed using the Shapiro–Wilk and Levene's tests, respectively. Appropriate ANOVA and post-hoc multiple comparison tests were applied as indicated in the figure legends. Data are presented as the mean ± standard deviation (SD) unless otherwise stated. Proportional data are presented as median with individual replicate points. Differences were considered statistically significant at a two-sided $p < 0.05$. Statistical significance was indicated as follows: ns, not significant; * $p < 0.05$; ** $p < 0.01$; *** $p < 0.001$; and **** $p < 0.0001$.

3. Results

3.1. Detection of Ghrelin Immunoreactivity in Immature COCs and Denuded Oocytes

Immunofluorescence staining revealed ghrelin-like immunoreactivity in both immature COCs and denuded oocytes (Figure 1). In intact COCs, ghrelin immunoreactivity was detected in the oocyte and surrounding cumulus-cell compartment. In denuded oocytes, ghrelin immunoreactivity was predominantly observed in the ooplasm. The primary-antibody-omission control showed no detectable specific fluorescence above background under the same staining and imaging conditions (Figure 1B,B′,D,D′). These findings support the detection of ghrelin-like immunoreactivity in immature bovine COCs and oocytes, supporting the possibility that local ghrelin signaling may participate in the regulation of bovine oocyte maturation.

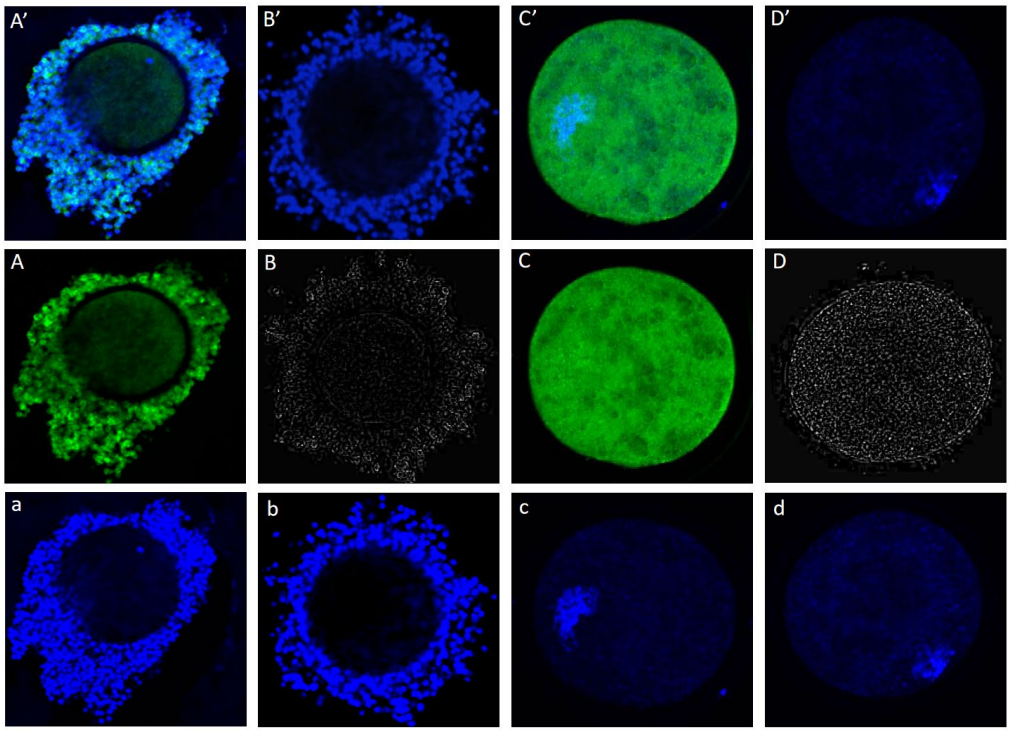


Figure 1. Immunofluorescence detection of ghrelin-like immunoreactivity in immature bovine COCs and denuded oocytes. (**A**,**A′**): Ghrelin immunoreactivity (green); (**B**,**B′**): Primary-antibody-omission negative control for ghrelin immunostaining; (**a**–**d**): Nuclear staining (blue, DAPI); (**C**,**C′**): Merged image of ghrelin immunoreactivity (green) and nuclear staining (blue); (**D**,**D′**): Merged image of negative control and nuclear staining. Representative images are shown from 150 COCs and 150 denuded oocytes examined across 3 independent experiments. The merged images show the distribution of ghrelin immunofluorescence relative to the nuclear staining. Primary-antibody-omission controls (**B**,**B′**,**D**,**D′**) were processed in parallel, with blocking solution substituted for the primary antibody; the secondary antibody and all other steps were retained. These controls were used to assess background fluorescence under the staining conditions. Scale bar = 50 μm, applicable to all panels. These immunofluorescence data demonstrate ghrelin-like immunoreactivity and do not provide quantitative or functional evidence.

3.2. Temporal Expression Profile of Ghrelin During Bovine Oocyte IVM

The temporal expression pattern of ghrelin mRNA was examined separately in cumulus cells and oocytes collected at 0, 6, 12, 18, and 24 h of IVM. Relative to the 0 h baseline, ghrelin expression in both cumulus cells and oocytes increased during the early phase of IVM, reached its highest level at 12 h, and subsequently declined from 12 to 24 h (Figure 2). In cumulus cells, ghrelin mRNA expression at 6, 12, and 18 h was significantly higher than that at 0 h ($p < 0.001$). A similar pattern was observed in oocytes, in which ghrelin expression was significantly elevated at 6, 12, and 18 h compared with that at 0 h ($p < 0.01$). The transient increase in ghrelin expression during the first half of IVM suggests that ghrelin may be involved in the dynamic molecular events associated with cumulus–oocyte complex maturation.

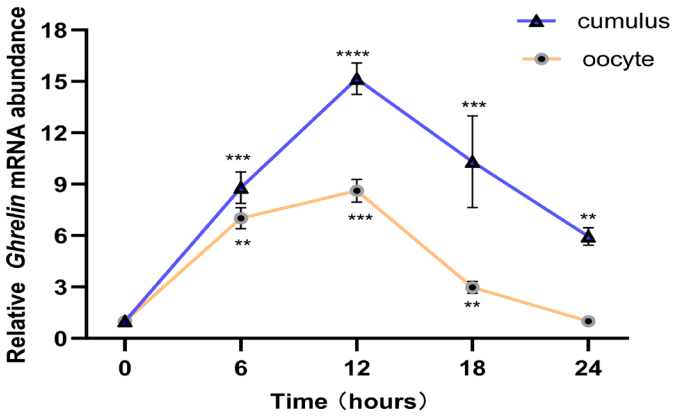


Figure 2. Temporal changes in relative *ghrelin* mRNA abundance in bovine cumulus cells and oocytes during IVM. COCs were collected at 0, 6, 12, 18, and 24 h of IVM. Following hyaluronidase treatment and pipetting, denuded oocytes were collected, while the corresponding cumulus cells were recovered by centrifugation. For each biological replicate and time point, 50 oocytes were pooled as one oocyte sample, and the cumulus cells obtained from the corresponding 50 COCs were pooled as one cumulus-cell sample. The two cell types were analyzed separately by qRT-PCR. Transcript levels were normalized to *GAPDH* and expressed relative to the corresponding 0 h samples within each cell type. Data are presented as the mean ± SD from 3 independent biological replicates. Asterisks indicate comparisons with the corresponding 0 h group within each cell type. Statistical significance was determined by one-way ANOVA followed by Dunnett's multiple comparison test.ns, not significant, ** $p < 0.01$, *** $p < 0.001$, and **** $p < 0.0001$.

3.3. Ghrelin Accelerates Bovine Oocyte Maturation and Enhances Maturation-Related Gene Expression

To evaluate whether ghrelin affects bovine oocyte maturation kinetics, COCs were cultured in control medium or medium supplemented with 50 ng/mL ghrelin. At 16 h of IVM, the first polar body extrusion rate in the G50 group was significantly higher than that in the time-matched control group (median, G50 16 h:67.47%; CON 16 h:32.47%; $p < 0.05$) (Figure 3a,b). No significant difference in the first polar body extrusion rate was observed between the G50 and control groups at 24 h. Representative images additionally showed more pronounced cumulus expansion in the G50 group at 16 h than in the time-matched control group. In parallel, ghrelin supplementation significantly increased the expression of the cumulus expansion-related gene *HAS2* in cumulus cells and the oocyte-derived growth factor genes GDF9 and BMP15 in denuded oocytes compared with the corresponding control group (Figure 3c; $p < 0.05$). Collectively, these results indicate that 50 ng/mL ghrelin accelerated nuclear maturation under the present IVM conditions and was associated with increased expression of genes related to cumulus expansion and oocyte developmental potential. However, the extrusion of the first polar body does not necessarily equate to full cytoplasmic maturation or enhanced developmental competence. Therefore, 16 h was selected as the sampling time for the ghrelin-treated group in subsequent mechanistic experiments.

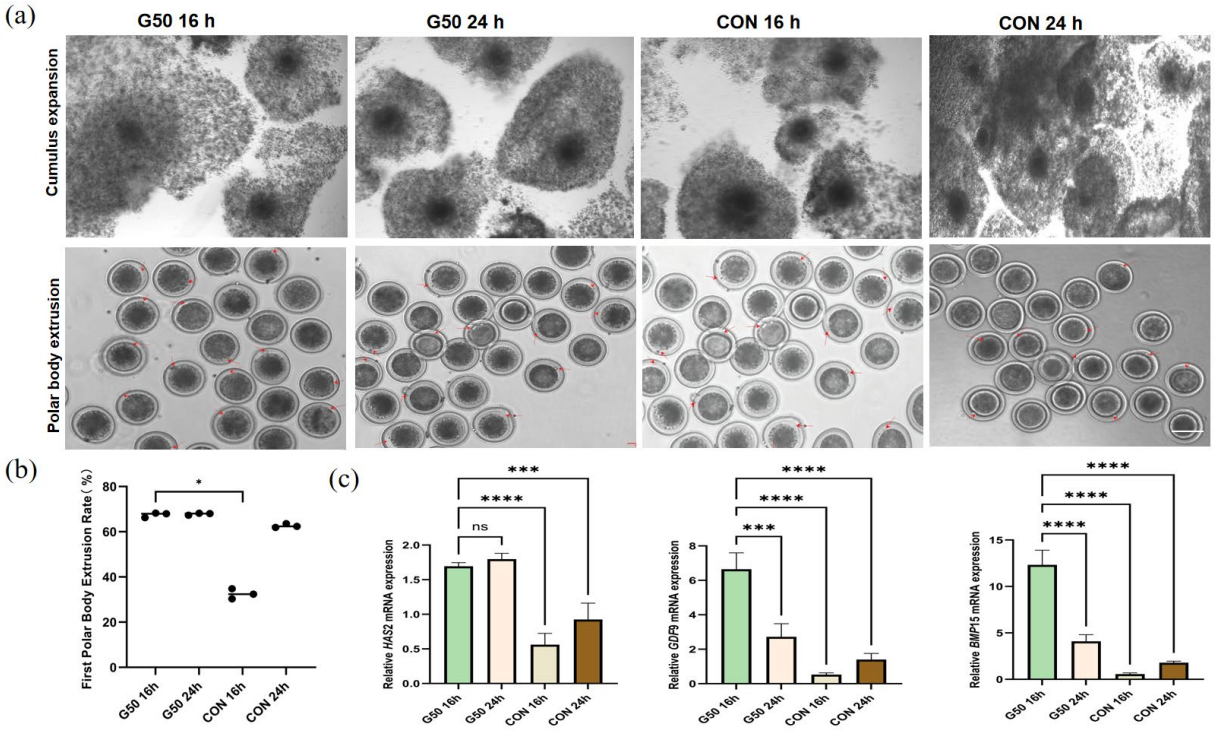


Figure 3. Effects of 50 ng/mL ghrelin on bovine oocyte maturation kinetics and maturation-related gene expression. (**a**) Representative images of COCs after IVM under the indicated treatment conditions. The arrow indicates the extruded first polar body. (**b**) First polar body extrusion rates after 16 and 24 h of IVM. Data are presented as median from three independent biological replicates ($n = 3$), with 50 oocytes per treatment group in each replicate. Statistical analysis was performed using Kruskal–Wallis test followed by Dunn's multiple comparisons test for comparisons of each of the other groups versus the G50 16 h group, and only these comparisons are shown. (**c**) Relative mRNA expression of *HAS2* in cumulus cells and *GDF9* and *BMP15* in denuded oocytes. Data are shown as mean ± SD, analyzed by one-way ANOVA followed by Dunnett's multiple comparisons test. ns, not significant, * $p < 0.05$, *** $p < 0.001$, and **** $p < 0.0001$. Scale bar = 50 μm in panel (**a**).

3.4. Transcriptomic Analysis: A Three-Level Comparative Framework

Quality-control metrics for the RNA-sequencing libraries, including clean-read numbers, Q30 values, and mapping rates, are summarized in Supplementary Table S2. Principal-component analysis and sample-correlation analysis showed good clustering of biological replicates within each experimental group and separation according to treatment and culture duration (Supplementary Figure S1). These results supported the consistency of the biological replicates and indicated that both ghrelin treatment and culture duration contributed to the overall transcriptomic variation. Differential expression and pathway enrichment analyses were first performed using the factorial DESeq2 model and were then complemented by three biologically motivated pairwise comparisons.

3.4.1. Isochronic Comparison: CON-16 h vs. G50-16 h

When culture duration was strictly matched at 16 h, the comparison between CON-16 h and G50-16 h identified 953 DEGs according to the predefined criteria. Functional enrichment analysis showed the top enriched biological processes included tRNA aminoacylation/amino acid activation (adjusted $p = 0.0148$) and cellular protein catabolic processes (adjusted $p = 0.0353$). Multiple aminoacyl-tRNA synthetases and several core proteasome subunits were upregulated in the ghrelin-treated group. These findings indicate that, at the same 16 h culture duration, ghrelin was associated with transcriptional changes in amino acid activation, translational preparation, and intracellular protein quality-control processes.

They are consistent with the possibility that ghrelin contributes to early cytoplasmic remodeling during IVM. However, this comparison does not by itself establish that these changes represent a complete maturation program or that they are independent of the interaction between treatment and culture duration. The comparison is presented in Supplementary Figure S2 and Table S3.

3.4.2. Time-Course Reference Comparison: Con-16 h vs. CON-24 h

The comparison between untreated control oocytes collected after 16 h and 24 h of IVM identified 774 DEGs. The most significantly enriched biological process was the oxidation–reduction process (GO:0055114; adjusted $p = 0.0440$), which involved 57 genes, including *HMOX1*, *G6PD*, *GPX1*, *PRDX1*, *GSR*, *TXNRD1*, *IDH1*, and other redox-related genes. Monosaccharide metabolic process and hexose metabolic process showed nominal enrichment but did not reach the predefined adjusted significance threshold. These findings indicate that redox-related transcriptional changes occur during the normal progression of bovine oocyte IVM from 16 h to 24 h. This comparison provides a time-course reference for interpreting the ghrelin-associated comparisons, particularly the comparison between G50-16 h and CON-16 h. However, it cannot by itself distinguish changes related to normal maturation progression from changes specifically associated with ghrelin treatment (Supplementary Table S4).

3.4.3. Maturation Phenotype-Based Comparison: G50-16 h Versus CON-24 h

The main effects of ghrelin treatment, culture duration, and their interaction were first evaluated using the factorial model, and the pairwise comparisons were performed as exploratory analyses. A factorial DESeq2 analysis was used to distinguish the main effects of ghrelin treatment, culture duration, and their interaction across the four experimental groups. The interaction analysis identified a significant ghrelin-by-time effect involving PI3K-Akt signaling (adjusted p-value < 0.05), indicating that the transcriptional response associated with this pathway differed between the 16 h and 24 h culture conditions. Because G50-16 h and CON-24 h oocytes exhibited comparable maturation phenotypes, a maturation phenotype-based exploratory comparison was performed between these two groups. Using the criteria of $|\log2 \text{ fold change}| > 1$ and an adjusted p-value < 0.05, this comparison identified 4515 DEGs, including 2570 upregulated and 1945 downregulated genes in G50-16 h relative to CON-24 h (Figure 4a).

Gene Ontology enrichment analysis showed that the upregulated DEGs were mainly associated with phosphorylation, oxidation–reduction processes, and proteolysis-related biological processes. Enriched molecular-function categories included molecular-function regulation and signaling-receptor activity. Downregulated DEGs were mainly associated with G protein-coupled receptor signaling, metabolic and biosynthetic processes, and extracellular-region-related categories (Figure 4b,c). KEGG pathway analysis showed that the upregulated DEGs were enriched in pathways related to cytochrome P450-mediated xenobiotic metabolism, GSH metabolism, amino acid biosynthesis, and PI3K-Akt signaling (Figure 4d). Downregulated DEGs were enriched in pathways including transforming growth factor-β signaling, neuroactive ligand–receptor interaction, and complement and coagulation cascades (Figure 4e). Although the color gradients in the bubble plots (Figure 4d,e) represent −log10 (raw p-value) to illustrate the significance distribution, pathways with an adjusted p-value < 0.05 were considered statistically significantly enriched. Several genes related to cellular signaling and survival, including FGF2, ARAF, VEGFA, IL4R, and ITGA7, were among the DEGs identified in this comparison.

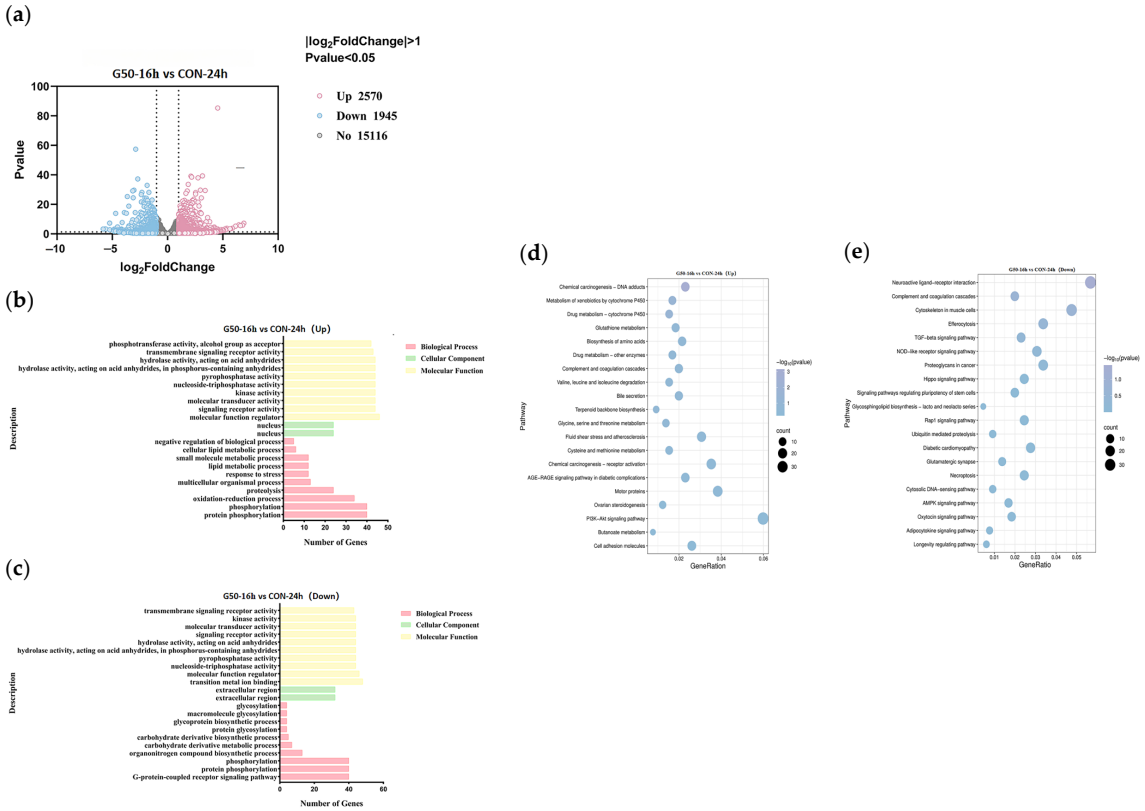


Figure 4. Transcriptomic analysis of MII-stage bovine oocytes from the G50-16 h and CON-24 h groups. (**a**) Volcano plot of differentially expressed genes (DEGs). Pink and blue dots indicate genes upregulated and downregulated, respectively, in G50-16 h relative to CON-24 h; gray dots indicate genes that did not meet the DEG criteria. DEGs were defined as genes with $|\log_2$ fold change$| > 1$ and a Benjamini–Hochberg-adjusted p value < 0.05 (For visualization purposes, the y-axis and the dashed lines display raw p values, as labeled in the figure). (**b**,**c**) Bar charts of Gene Ontology (GO) functional enrichment for upregulated and downregulated DEGs, respectively. (**d**,**e**) Bubble plots of Kyoto Encyclopedia of Genes and Genomes (KEGG) pathway enrichment for upregulated and downregulated DEGs, respectively. GO terms and KEGG pathways with an adjusted p value < 0.05 were considered significantly enriched. In the bubble plots, the x-axis represents the GeneRatio, bubble size indicates the number of enriched genes, and color represents $-\log_{10}$ (raw p value) to illustrate the overall significance distribution, whereas statistical significance is strictly based on the adjusted p value.

In the phenotype-based comparison, the PI3K-Akt signaling pathway exhibited the highest GeneRatio and the largest number of enriched genes, whereas the GSH metabolism pathway was the most significantly enriched metabolic pathway. These pathways represented prominent molecular features distinguishing the transcriptional states of G50-16 h and CON-24 h oocytes. Together, these findings support the hypothesis that ghrelin may influence maturation-associated signaling and redox regulation during IVM. However, because the phenotype-based comparison involved differences in both treatment and culture duration, these results should be interpreted as pathway features associated with the respective transcriptional states rather than as evidence that ghrelin treatment alone recapitulates the molecular or redox state of 24 h control oocytes at 16 h.

Given the prominent enrichment of the PI3K-Akt signaling pathway, and its reported roles in mammalian oocyte maturation and cell-survival regulation, we next used LY294002 as a pharmacological intervention to examine the potential contribution of this pathway to ghrelin-associated responses. The effects of LY294002 on ghrelin-associated changes in the expression of VEGFA, FGF2, BAX, and BCL-2 were then evaluated.

3.5. Effects of LY294002 Treatment on Nuclear Maturation and Apoptosis-Related Gene Expression

The PI3K-Akt inhibitor LY294002 was first evaluated at concentrations of 0, 5, 10, 15, and 20 μM to determine an appropriate concentration for pathway-intervention experiments. After 24 h of IVM, treatment with 5, 10 or 15 μM LY294002 did not significantly affect first polar body extrusion compared with the vehicle control. A significant reduction in first polar body extrusion was observed at 20 μM relative to the 0 μM control group (median, control 0 μM:65.21%; 20 μM:49.05%; $p < 0.01$) (Figure 5b). We further detected the mRNA levels of oocyte maturation-related genes. The mRNA abundance of *HAS2* and *GDF9* was unchanged in the 5 μM group compared with the control, while 10 μM LY294002 significantly decreased the expression of *HAS2* and *GDF9*. Higher concentrations (15 and 20 μM) further reduced the transcript levels of *HAS2* and *GDF9* (Figure 5c,d). Although 20 μM LY294002 significantly reduced first polar body extrusion, this concentration was not selected because the reduction in nuclear maturation itself would confound interpretation of downstream gene expression. At 10 μM, *HAS2* and *GDF9* expression was significantly decreased without a significant change in first polar body extrusion, allowing pathway-associated transcriptional effects to be assessed independently of altered nuclear maturation. Taken together, 10 μM LY294002 was selected for subsequent experiments: at this concentration, the inhibitor significantly downregulated maturation-related gene expression without altering the first polar body extrusion rate, thereby avoiding the confounding effect of impaired nuclear maturation.

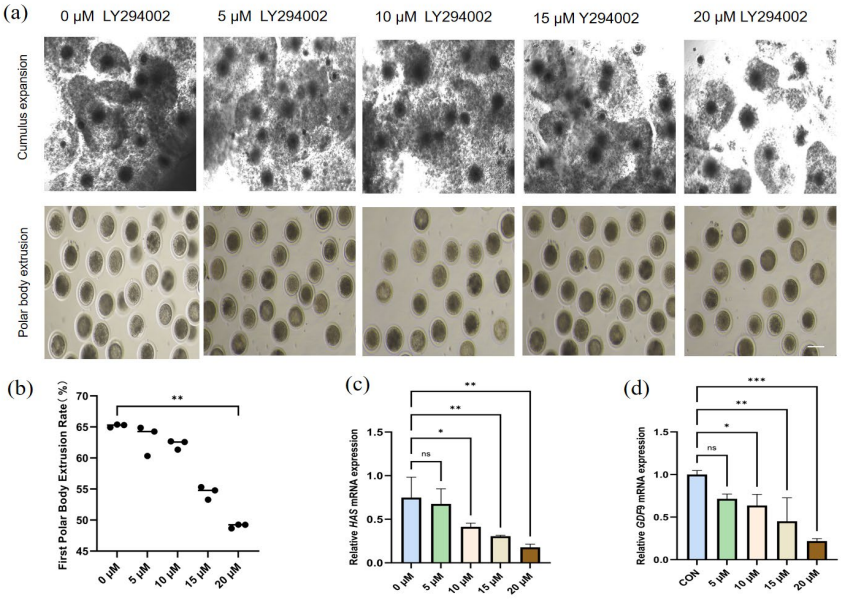


Figure 5. Effects of LY294002 on bovine oocyte nuclear maturation. (**a**) Representative images showing cumulus expansion (**upper row**) and first polar body extrusion (**lower row**) after 24 h of IVM in the presence of 0, 5, 10, 15, or 20 μM LY294002. (**b**) Quantification of first polar body extrusion rates. Data for panel (**b**) are presented as median values with individual data points from three independent biological replicates ($n = 3$), with 50 oocytes per treatment group in each replicate. Statistical analysis for panel (**b**) was performed using the Kruskal–Wallis test followed by Dunn's multiple comparisons test, with all comparisons only versus the 0 μM LY294002 control group. (**c**) Relative mRNA expression of HAS2 in cumulus cells. (**d**) Relative mRNA expression of GDF9 in denuded oocytes. Data in panels (**c**,**d**) are shown as mean ± SD from three independent biological replicates ($n = 3$). Statistical analysis for panels (**c**,**d**) was performed using one-way ANOVA followed by Dunnett's multiple comparisons test, with each LY294002 treatment group compared with the 0 μM LY294002 control group. ns, not significant; * $p < 0.05$, ** $p < 0.01$, *** $p < 0.001$. Scale bar = 50 μm in panel (**a**).

To further investigate whether the ghrelin-associated acceleration of nuclear maturation was dependent on PI3K-Akt signaling, the first polar body extrusion rate was evaluated in the presence of LY294002 (Figure 6a). All four treatment groups were measured within the same experimental batches, and paired nonparametric pairwise comparisons with Holm adjustment were performed for all six pairwise comparisons. No statistically significant difference in first polar body extrusion rate was detected between the CON and G50 groups, between the CON and LY294002 groups, between the G50 and LY294002 groups, or between the LY294002 + G50 group and any of the other three groups (all adjusted $p > 0.05$). Because no significant pairwise difference was detected in this experiment, these data do not provide statistical evidence that LY294002 modified the ghrelin-associated maturation response, and the pharmacological evidence for PI3K-Akt involvement remains inconclusive. The limited number of biological batches ($n = 3$) may have restricted the power to detect moderate differences, and this experiment should therefore be interpreted together with the transcriptional and gene-expression data rather than as independent functional proof.

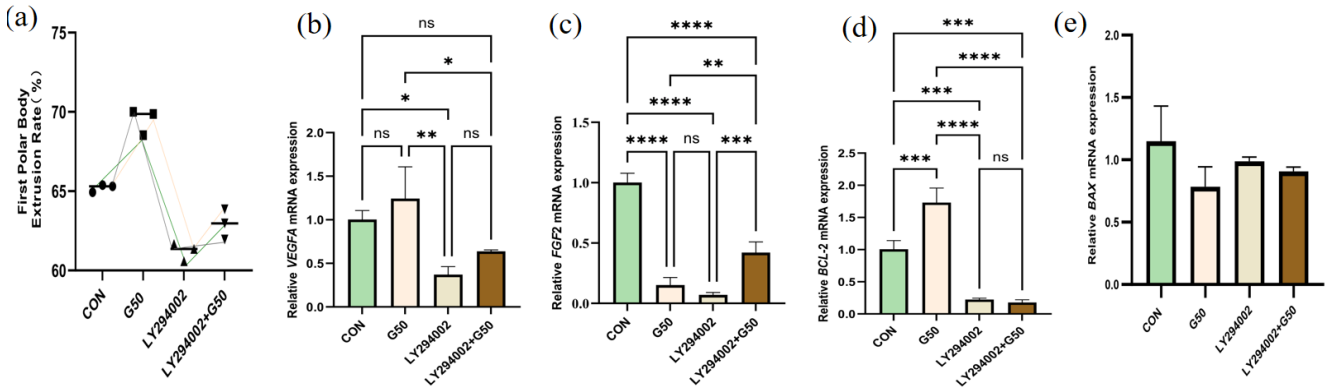


Figure 6. Effects of ghrelin and LY294002 on the first polar body extrusion rate and relative mRNA expression of PI3K-Akt-associated and apoptosis-related genes in bovine oocytes. (**a**) First polar body extrusion rate; (**b**) *VEGFA*; (**c**) *FGF2*; (**d**) *BCL-2*; and (**e**) *BAX*. CON, vehicle control; G50, 50 ng/mL ghrelin; LY294002, 10 μM LY294002; LY294002 + G50, co-treatment with LY294002 and ghrelin. For panel (**a**), First polar body extrusion rate (%) after 16 h of IVM. Data are presented as median with individual biological replicates ($n = 3$ independent batches; 50 oocytes per group per batch; all four groups measured within each batch). The biological replicate was the statistical unit; individual oocytes were not independent replicates. Pairwise comparisons used two-sided Wilcoxon matched-pairs signed-rank tests with Holm adjustment for all six pairwise comparisons among the four groups (CON, G50, LY294002, and LY294002 + G50). No comparison was significant after Holm adjustment (all adjusted $p > 0.05$; ns). For panels (**b**–**e**), comparisons between specific groups are indicated by brackets. ns, not significant, * $p < 0.05$, ** $p < 0.01$, *** $p < 0.001$, and **** $p < 0.0001$.

The effects of ghrelin and PI3K-Akt inhibition on the expression of selected survival- and apoptosis-related genes were subsequently examined in oocytes cultured for 16 h. VEGFA expression did not differ significantly between the CON and G50 groups, whereas LY294002 treatment significantly decreased *VEGFA* expression relative to both groups ($p < 0.05$). Co-treatment with ghrelin partially increased VEGFA expression compared with LY294002 alone but did not restore expression to the control level (Figure 6b). *FGF2* expression was significantly lower in both the G50 and LY294002 groups than in the CON group, while the LY294002 + G50 group showed higher *FGF2* expression than either the G50 or LY294002 group but remained lower than the CON group (Figure 6c). In addition, *BCL-2* expression was significantly increased by ghrelin treatment, whereas LY294002 alone or in combination with ghrelin reduced *BCL-2* expression relative to the G50 group (Figure 6d). *BAX* expression was numerically lower in the G50 group and numerically higher after LY294002 treatment, but these differences did not reach statistical significance. (Figure 6e).

Overall, PI3K-Akt inhibition altered ghrelin-associated expression patterns of *VEGFA*, *FGF2*, *BCL-2*, and *BAX*. In particular, the loss of ghrelin-associated *BCL-2* upregulation following LY294002 treatment supports the involvement of PI3K-Akt signaling in the regulation of this anti-apoptotic transcriptional response. However, because only mRNA expression was evaluated, these findings do not directly establish changes in PI3K-Akt phosphorylation or apoptosis rates.

3.6. Ghrelin Improves Intracellular Redox Homeostasis and Organelle-Related Fluorescence Parameters

Given that the GSH metabolism was significantly enriched among the pathways associated with upregulated DEGs, intracellular GSH and ROS levels were evaluated in mature oocytes. Compared with the CON group, oocytes treated with 50 ng/mL ghrelin exhibited significantly higher CellTracker Blue fluorescence intensity, indicating increased intracellular GSH-associated fluorescence (G50: 43.008 ± 1.15; CON: 34.600 ± 0.27; $p = 0.0250$) (Figure 7a,b). In contrast, ROS-associated fluorescence was significantly lower in the G50 group than in the control group (G50: 9.772 ± 0.52; CON: 13.609 ± 0.42; $p = 0.0111$) (Figure 7a,c). These findings demonstrate that ghrelin treatment was associated with altered intracellular redox profile during bovine oocyte IVM.

MitoTracker Red CMXRos fluorescence intensity was significantly increased in the G50 group relative to the CON group ($p < 0.05$), and LysoTracker Red fluorescence intensity was also significantly higher after ghrelin treatment ($p < 0.05$) (Figure 7a,d,e). These results indicate that ghrelin altered mitochondrial and lysosomal fluorescence parameters in mature bovine oocytes. Since MitoTracker and LysoTracker fluorescence signals are influenced by probe accumulation, membrane potential, and staining conditions, the present findings are interpreted as changes in organelle-related fluorescence intensity and distribution rather than direct evidence of increased mitochondrial or lysosomal number, biogenesis, or functional activity.

Furthermore, DAPI chromosome staining was performed to assess the meiotic maturation status of PB-extruded oocytes. The proportion of PB-extruded oocytes reaching a normal MII chromosome configuration did not differ significantly between the G50 and CON groups ($p > 0.05$; Figure 7f). This endpoint differs from the first polar body extrusion rate shown in Figure 3b: Figure 3b uses all morphologically intact oocytes as the denominator and reflects the kinetics of nuclear maturation, whereas Figure 7f uses PB-extruded oocytes as the denominator and reflects the chromosomal quality of oocytes that have already completed polar body extrusion. Thus, the higher 16 h extrusion rate in the G50 group and the comparable MII configuration proportion among PB-extruded oocytes are not contradictory. A fraction of PB-extruded oocytes in both groups failed to establish a normal MII configuration, indicating that first polar body extrusion alone is not a complete indicator of MII chromosome quality.

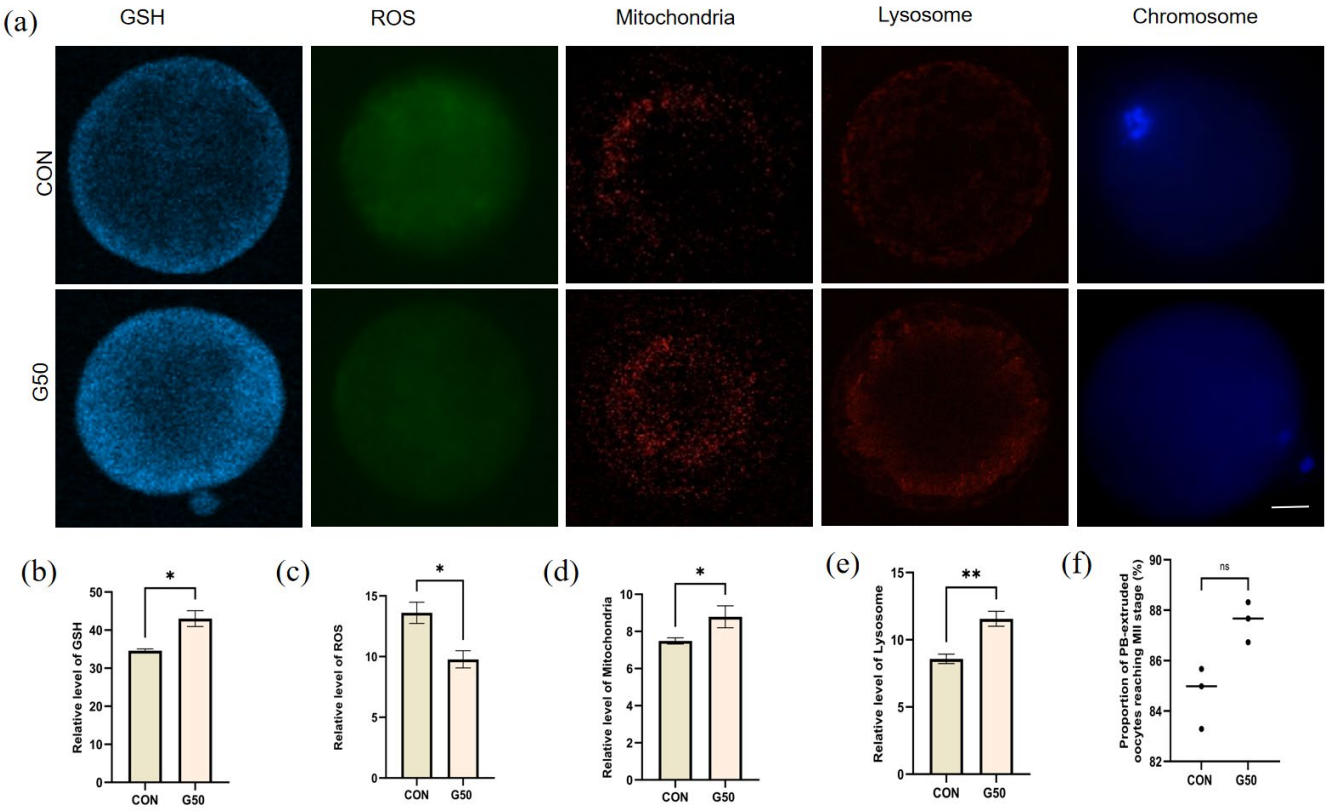


Figure 7. Comparison of redox-related and organelle fluorescence parameters and MII status between G50-16 h and CON-24 h bovine oocytes. (**a**) Representative confocal images of intracellular GSH, ROS, MitoTracker Red CMXRos, and LysoTracker Red staining in CON and G50 groups. (**b**–**e**) Quantitative analysis of relative fluorescence intensity for GSH, ROS, mitochondrial, and lysosomal staining, respectively. (**f**) Proportion of PB-extruded oocytes reaching MII stage (%). Note that this endpoint uses PB-extruded oocytes as the denominator and is therefore not directly comparable to the first polar body extrusion rate in Figure 3b. The statistical unit in all panels was the biological replicate, not the individual oocyte. For panels (**b**–**e**), data are presented as the mean ± SD from three independent biological replicates ($n = 3$), with 50 oocytes per treatment group in each replicate, and analyzed by a paired two-tailed t-test. For panel (**f**), the percentage was calculated for each biological replicate and is presented as median with individual data points ($n = 3$); because the proportional data did not meet the normality assumption for parametric tests, a paired non-parametric test (Wilcoxon signed-rank test) was used. Asterisks indicate significant differences compared with the CON group. ns, not significant, * $p < 0.05$, ** $p < 0.01$. Scale bar = 25 µm in panel (**a**).

3.7. Ghrelin Improves Mitochondrial Membrane Potential

Mitochondrial membrane potential was assessed using the JC-1 fluorescent probe. Compared with oocytes in the CON group, oocytes in the G50 group exhibited a significantly stronger red JC-1 aggregate signal and a significantly weaker green JC-1 monomer signal (Figure 8a). Quantitative analysis further showed that the relative level of JC-1 monomers was significantly decreased ($p < 0.01$) (Figure 8b), whereas the relative level of JC-1 aggregates was significantly increased in the G50 group ($p < 0.001$) (Figure 8c). These results suggest that ghrelin treatment was associated with an improved mitochondrial membrane-potential status in bovine oocytes matured in vitro. Together with the increased GSH-associated fluorescence and decreased ROS-associated fluorescence, these findings suggest that ghrelin treatment may contribute to the maintenance of mitochondrial homeostasis during bovine oocyte IVM.

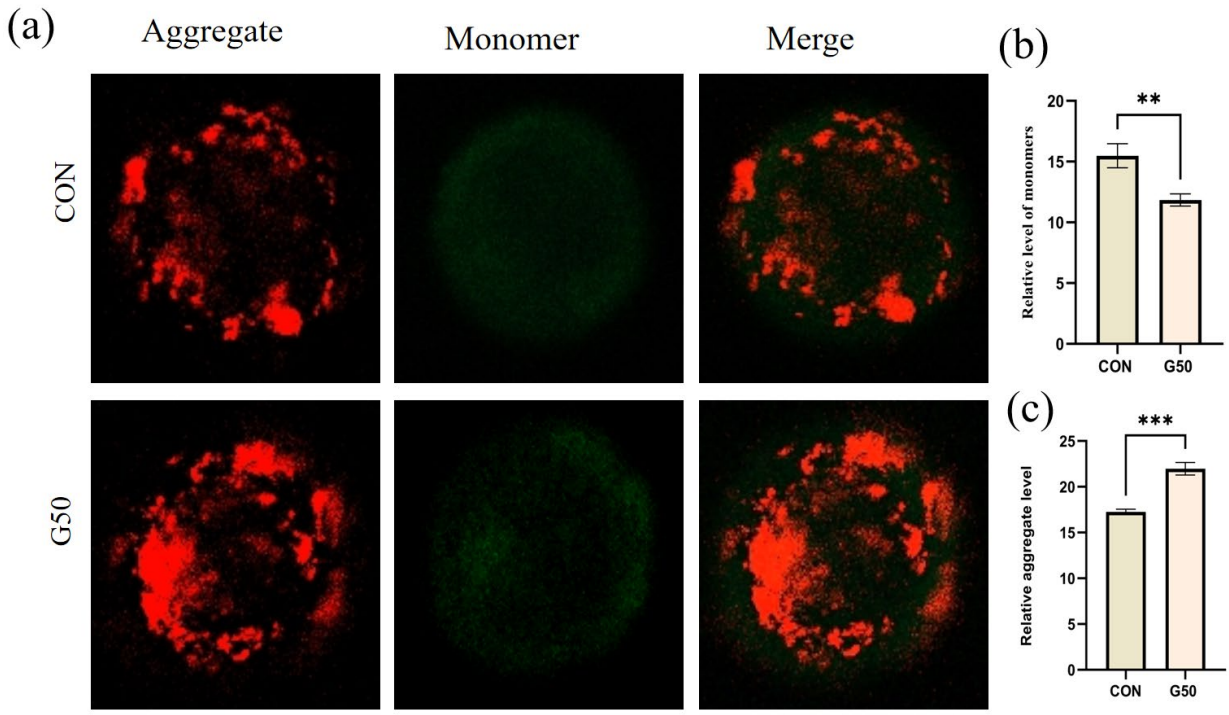


Figure 8. Effects of 50 ng/mL ghrelin on mitochondrial membrane potential in mature bovine oocytes. (**a**) Representative JC-1 fluorescence images. JC-1 aggregates are shown in red, and JC-1 monomers are shown in green. (**b**) Quantification of the relative JC-1 monomer level. (**c**) Quantification of the relative JC-1 aggregate level. Data are presented as the mean ± SD from 3 independent biological replicates, with 50 oocytes per treatment group in each replicate. For each oocyte, the JC-1 red/green fluorescence ratio was calculated; within each biological replicate, these values were averaged for each group. These replicate-level means were then used for statistical analysis. The statistical unit was the biological replicate, not the individual oocyte. Statistical analysis was performed using a paired *t*-test (two-tailed). Asterisks indicate significant differences compared with the CON group. ** $p < 0.01$, *** $p < 0.001$.

4. Discussion

4.1. Ghrelin Immunoreactivity and Dynamic Ghrelin Transcript Levels Are Detected During Bovine Coc Maturation

IVM is an essential step in bovine in vitro embryo production; however, oocytes matured in vitro generally exhibit lower developmental competence than those matured within the follicular environment. This discrepancy is associated with incomplete cytoplasmic maturation, suboptimal cumulus–oocyte communication, mitochondrial dysfunction, and excessive accumulation of ROS during culture [3,23]. Therefore, identifying endogenous follicular factors that can improve the coordination between nuclear and cytoplasmic maturation remains an important objective in bovine reproductive biotechnology.

In the present study, ghrelin-like immunoreactivity was detected in both immature COCs and the cytoplasm of oocytes, suggesting that ghrelin may play a functional role in COCs. This observation is consistent with previous evidence showing that ghrelin and its receptor are expressed in bovine oocytes and cumulus cells [24]. In addition, relative ghrelin mRNA abundance showed a time-dependent pattern during IVM, increasing during the early and intermediate stages of culture, reaching the highest observed level at 12 h, and subsequently decreasing by 24 h.

Both the control and ghrelin-treated groups retained the endogenous ghrelin background. Therefore, the present study compared oocytes cultured without additional ghrelin

supplementation with those cultured with exogenous ghrelin supplementation, rather than comparing ghrelin-deficient and ghrelin-replete conditions.

Interpretation of the ghrelin mRNA profile in oocytes requires consideration of the transcriptional quiescence associated with meiotic maturation. Bovine oocytes exhibit markedly reduced transcriptional activity as meiosis resumes, particularly following germinal vesicle breakdown. Therefore, the higher relative ghrelin mRNA level observed at 12 h should not be interpreted as evidence of de novo ghrelin transcription. Because the qRT-PCR measurements were normalized to GAPDH, they reflect relative transcript abundance rather than absolute transcript copy numbers per oocyte. Differential turnover of pre-existing maternal transcripts, together with changes in the abundance of the reference transcript, could contribute to the observed profile. However, these possibilities were not directly assessed, and the mechanism underlying the increase remains unresolved. Cumulus cells do not undergo the same meiotic transcriptional silencing as oocytes; therefore, the profiles of these two cell types should be interpreted separately. These qRT-PCR results describe temporal changes in relative ghrelin mRNA abundance but do not establish increased ghrelin transcription, protein production, or secretion.

4.2. Ghrelin Accelerates Nuclear Maturation While Supporting Maturation-Related Gene Expression

The present results showed that supplementation with 50 ng/mL ghrelin increased first polar body extrusion after 16 h of IVM. Previous studies have examined the effects of ghrelin supplementation on oocyte maturation and related signaling in bovine and sheep IVM systems [25–27]. Because first polar body extrusion is a proportional endpoint, rates were analyzed using nonparametric tests and are reported as medians. At 16 h, the median first polar body extrusion rate was higher in the G50 group than in the time-matched control group (G50 16 h, 67.47% vs. CON 16 h, 32.47%; $p < 0.05$, Kruskal–Wallis test followed by Dunn's multiple-comparison test). At 24 h, no significant difference was detected between the G50 and control groups. These findings suggest that ghrelin accelerated meiotic maturation under the present culture conditions.

The rate of first polar body extrusion is widely regarded as the gold standard for evaluating oocyte nuclear maturation, but it does not necessarily reflect the completion of cytoplasmic maturation or the acquisition of full developmental competence. We therefore examined *HAS2*, *GDF9*, and *BMP15*, which are functionally associated with cumulus expansion, oocyte–cumulus communication, and oocyte developmental competence. Ghrelin treatment increased the expression of these genes at the selected sampling time, suggesting that the accelerated nuclear maturation was accompanied by molecular changes in the COCs compartment. *HAS2* encodes hyaluronan synthase 2, a key enzyme involved in the synthesis of hyaluronan during cumulus expansion, whereas *GDF9* and *BMP15* encode oocyte-secreted factors that regulate cumulus-cell function and follicular communication [28,29]. These results support the interpretation that ghrelin may promote a more coordinated maturation process rather than merely inducing premature meiotic progression. However, because fertilization and embryo-development outcomes were not evaluated in the present study, the developmental significance of the observed gene-expression changes remains to be confirmed.

The selection of 16 h as the sampling point for ghrelin-treated oocytes allowed comparison with conventionally matured oocytes collected at 24 h, when the two groups showed comparable or higher maturation-related phenotypes. This experimental design was useful for identifying molecular pathways associated with accelerated maturation. Nevertheless, the comparison between 16 h-treated and 24 h-control oocytes also includes a difference in culture duration. Consequently, the transcriptomic findings should be interpreted as

pathways associated with the ghrelin-induced accelerated maturation phenotype, rather than as exclusively ghrelin-dependent changes independent of maturation time.

4.3. Association of PI3K-Akt Signaling with Ghrelin-Related Maturation and Survival-Related Transcriptional Responses

4.3.1. Strengths and Interpretation of the Multi-Layer Transcriptomic Design

A potential limitation of a simple two-group comparison between oocytes collected at 16 h and 24 h is that any observed difference could reflect time-dependent transcriptomic drift rather than a specific treatment effect. In the present study, this issue was substantially mitigated by the inclusion of a complete 2 × 2 factorial RNA-seq dataset across all four time and treatment combinations. The strictly isochronic 16 h comparison demonstrated that ghrelin itself can rapidly activate tRNA aminoacylation, amino acid activation and protein catabolic pathways within a fixed culture duration, revealing a direct transcriptional effect of the peptide. The 16 h–24 h control time-course comparison further provided empirical evidence that the full transcriptional establishment of oxidation–reduction and GSH-related signatures is not instantaneous in IVM, but instead represents a normal time-delayed maturation program that control oocytes require approximately 24 h to complete.

When these two independent levels of evidence are integrated with the main maturation phenotype-based comparison between G50-16 h and CON-24 h, the resulting pathway enrichment of PI3K-Akt signaling and GSH metabolism can no longer be explained purely by residual differences in maturation duration. The most parsimonious interpretation is that ghrelin is associated with the accelerated acquisition of a mature, redox-defended oocyte state, so that many of the molecular states that control oocytes would normally only reach after 24 h of culture appear to be already established in 16 h ghrelin-treated oocytes while they simultaneously show a higher first polar body extrusion rate. This three-level transcriptomic framework therefore provides stronger evidence that ghrelin coordinates pro-maturation and antioxidative transcriptional programs, rather than merely inducing a trivial or time-dependent experimental artifact.

4.3.2. Functional Implications of PI3K-Akt Signaling

PI3K-Akt signaling was enriched in the G50-16 h versus CON-24 h comparison, but this comparison differed in both treatment and culture duration, and transcript enrichment does not establish pathway activation. Akt phosphorylates PDE3A to promote cAMP hydrolysis and meiotic resumption [30], and PKA–Cdc2/cyclin B regulation further contributes to meiotic progression [31]. PI3K-Akt has been linked to mitochondrial function, apoptosis, and oxidative-stress responses [15,16,32,33]. However, ghrelin modulates Akt1 and ERK1/2 phosphorylation during bovine oocyte IVM in a time-dependent manner [26], and phospho-Akt was not measured here; PI3K-Akt therefore remains a candidate pathway.

LY294002 is not exclusively selective for PI3K [34]. In the concentration screen, 20 μM reduced first polar body extrusion, whereas 10 μM decreased HAS2 and GDF9 expression without significantly altering extrusion and was therefore used for intervention. In the four-group experiment (Figure 6a), however, no pairwise difference in first polar body extrusion was significant (all adjusted $p > 0.05$). These pharmacological data therefore do not demonstrate that PI3K-Akt mediates the ghrelin response and are best regarded as hypothesis-generating.

VEGFA and FGF2 responded differently, arguing against a single downstream mechanism. Although VEGFA is expressed in ovarian tissue and has been associated with follicular function [35], its role in isolated COCs during IVM remains unclear. FGF2/FGFR signaling has been implicated in cumulus expansion and meiotic progression in COCs [36], yet G50 oocytes showed lower FGF2 mRNA but higher HAS2, GDF9 and BMP15 expression

and accelerated maturation, indicating that FGF2 transcript level is not a simple readout of FGF2/FGFR output. PI3K-Akt/MAPK-ERK crosstalk and maturation-stage-dependent transcription may contribute, but this remains speculative without phospho-Akt and phospho-ERK1/2 data.

4.4. Ghrelin Is Associated with a More Favorable Apoptotic and Redox State

The relative expression of pro-apoptotic and anti-apoptotic genes is closely related to oocyte survival and developmental competence. In the present study, ghrelin treatment significantly increased *BCL-2* mRNA expression, whereas *BAX* mRNA expression was numerically lower, although this difference was not statistically significant. LY294002 was associated with reduced BCL-2 expression, whereas BAX expression was numerically higher but not significantly different. Taken together, these findings indicate that PI3K-Akt inhibition may weaken the anti-apoptotic gene-expression pattern associated with ghrelin treatment. The findings are consistent with the established role of Akt signaling in promoting cell survival through regulation of *BCL*-2 family proteins and suppression of mitochondrial apoptotic signaling [15,33]. However, because only *BCL*-2 and *BAX* mRNA expression was measured, these findings should be interpreted as changes in apoptosis-related gene expression rather than direct evidence of altered apoptosis, oocyte survival, or developmental competence.

The transcriptomic analysis also revealed significant enrichment of GSH metabolism among genes upregulated in ghrelin-treated oocytes. This finding was supported by the fluorescence analysis, which showed increased GSH fluorescence and reduced ROS fluorescence after ghrelin treatment (CON:13.609 ± 0.42, G50:9.772 ± 0.52, $p = 0.0111$). GSH is a major intracellular non-enzymatic antioxidant in mammalian oocytes and is essential for maintaining redox homeostasis during IVM. In bovine oocytes, higher GSH levels after maturation are associated with improved cytoplasmic maturation and enhanced developmental competence [9]. Conversely, excessive ROS can impair spindle organization, mitochondrial activity, membrane integrity, and embryo development [5]. Therefore, the simultaneous increase in GSH fluorescence and decrease in ROS fluorescence suggests that ghrelin is associated with a more favorable intracellular redox balance. However, since these assessments were performed at different time points (16 h vs. 24 h), the specific contribution of ghrelin independent of culture time cannot be fully delineated.

4.5. Ghrelin Is Associated with Altered Mitochondrial and Lysosomal Status

Mitochondria provide the ATP required for spindle assembly, chromosome segregation, cytoplasmic remodeling, and other energy-demanding events during oocyte maturation. Oocytes may be especially vulnerable to mitochondrial impairment because they contain numerous mitochondria, whereas the capacity to replace damaged organelles during maturation is limited [37,38]. In the present study, ghrelin-treated oocytes exhibited stronger MitoTracker Red CMXRos fluorescence than the control oocytes. In addition, the red-to-green fluorescence ratio obtained from the JC-1 assay was significantly higher following ghrelin treatment. Together, these findings indicate that ghrelin was associated with increased mitochondrial-associated fluorescence and a more favorable mitochondrial membrane-potential profile.

Mitochondrial membrane potential is an important component of oxidative phosphorylation and ATP production. However, fluorescence-based measurements of mitochondrial status require cautious interpretation. The accumulation of MitoTracker is affected by the mitochondrial membrane potential, whereas the JC-1 signal can vary with probe loading, the formation of fluorescent aggregates, and the imaging conditions. Therefore, the present findings support an association between ghrelin treatment and improved mitochondrial

functional status, but they do not directly demonstrate increased ATP production, mitochondrial biogenesis, or enhanced respiratory activity. Measurements of ATP content, oxygen consumption rate, mitochondrial ultrastructure, mitochondrial DNA copy number, and mitochondrial distribution would strengthen this conclusion. In addition, the preservation of MMP may be related to the observed changes in ROS and *BCL-2*/*BAX* expression, because mitochondrial depolarization can promote cytochrome c release and activation of the intrinsic apoptotic pathway.

Supplementation with ghrelin also increased LysoTracker Red fluorescence. Lysosomes participate in the degradation of damaged proteins and organelles and are functionally linked to autophagy, mitochondrial quality control, and cellular stress adaptation [39]. The increase in LysoTracker-associated fluorescence may therefore indicate altered lysosomal activity or acidification during ghrelin-associated maturation. However, fluorescence intensity alone cannot distinguish increased lysosomal mass from enhanced lysosomal acidification or altered probe accumulation. Direct evaluation of autophagic flux, lysosomal-associated membrane proteins, cathepsin activity, and mitophagy-related markers will be necessary to establish whether ghrelin activates lysosome-dependent quality-control pathways. Taken together, the current data suggest that ghrelin may coordinate redox regulation with mitochondrial and lysosomal homeostasis, thereby creating a more favorable cytoplasmic environment for oocyte maturation.

4.6. Synthesis of the Observed Findings

Taken together, the multiple lines of evidence presented in this study integrate phenotypic, transcriptomic, pharmacological, and fluorescence-based observations describing the biological outcomes following exogenous ghrelin supplementation during bovine COC IVM. At 16 h of in-vitro culture, ghrelin accelerates oocyte nuclear maturation and increases transcript abundance of cumulus-oocyte communication-related genes HAS2, GDF9, and BMP15. Transcriptome enrichment and inhibitor-intervention results point to the PI3K-Akt cascade as a candidate associated pathway that may contribute to anti-apoptotic transcriptional responses, even though direct pathway activation could not be confirmed in the present work. In parallel, ghrelin-treated oocytes display improved redox homeostasis, higher mitochondrial membrane potential, as well as modified mitochondrial and lysosomal fluorescence signatures. These coordinated cellular changes are summarized schematically in Figure 9. It should be emphasized that this schematic integrates correlative findings rather than establishing causal mechanistic relationships; critical unresolved points are outlined in the subsequent limitations section.

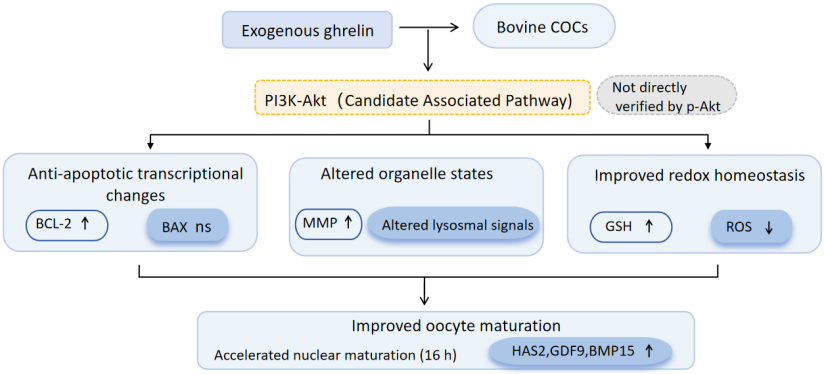


Figure 9. Schematic summary synthesizing observed effects of exogenous ghrelin during in vitro maturation of bovine COCs. Upward arrows indicate promotion, and downward arrows indicate inhibition.

Furthermore, the novelty of these findings lies in proposing a hierarchical regulatory model for ghrelin in the bovine model. Practically, these results suggest that supplementing IVM media with ghrelin could be a promising strategy to accelerate nuclear maturation and enhance the cytoplasmic quality of bovine oocytes, thereby potentially improving the efficiency of in vitro embryo production in livestock. Additionally, given the conserved nature of these pathways, targeting ghrelin signaling may offer translational insights for human assisted reproductive technologies (ART).

4.7. Limitations and Future Perspectives

Several limitations should be considered when interpreting the present findings. First, although ghrelin-like immunoreactivity was detected in COCs and oocytes and its expression varied during IVM, the upstream receptor-mediated mechanism was not directly examined. We have not confirmed whether the ghrelin receptor GHSR1a mediates the observed phenotypes; its functional involvement needs verification via GHSR1a protein detection, receptor-antagonist treatment or receptor-specific knockdown assays. Moreover, even if GHSR1a signalling contributes to the response, we cannot discriminate whether ghrelin acts directly on oocytes or exerts its effects indirectly via paracrine signalling from cumulus cells. In the absence of receptor-blocking evidence, any mechanistic model describing ghrelin action on bovine oocyte maturation remains speculative and requires further unequivocal functional validation.

Second, LY294002 was the main pharmacological approach used to examine the possible involvement of PI3K-Akt signaling. Although treatment with this inhibitor did not produce a statistically significant change in first polar body extrusion, it changed the expression of several genes, these findings alone do not demonstrate pathway specificity. This limitation could be addressed by examining the phosphorylation status of key components of the PI3K-Akt pathway, particularly phospho-Akt, together with complementary approaches such as Akt inhibition, siRNA-mediated gene silencing, or receptor blockade. The relationship between ghrelin and GSH metabolism also remains to be clarified. Direct biochemical assessment of GSH-related parameters, combined with the analysis of antioxidant-pathway markers, would provide additional evidence. Such experiments may help determine whether PI3K-Akt signaling and GSH metabolism act as separate mechanisms or as interconnected components of a broader ghrelin response.

Third, the present analysis was limited mainly to maturation rate, gene expression, fluorescence-based parameters, and mitochondrial membrane potential. Fertilization, cleavage, blastocyst formation, blastocyst cell number, apoptosis, and developmental competence after embryo transfer were not examined. These outcomes are needed to establish whether ghrelin-induced maturation produces developmentally competent oocytes, rather than simply promoting earlier polar body extrusion. Further work should therefore follow oocytes treated with ghrelin through in vitro fertilization and subsequent embryo development.

Fourth, a primary-antibody-omission negative control was included (Figure 1B,B′,D,D′), which showed no detectable specific fluorescence above background. However, isotype-matched IgG and antigen pre-adsorption controls were not performed in the present study. Accordingly, these immunofluorescence data are interpreted as evidence of ghrelin-like immunoreactivity rather than definitive proof of antibody specificity. Future studies should incorporate isotype and antigen pre-adsorption controls to further validate antibody specificity.

In addition, a large proportion of the OPU collections were performed during summer. Seasonal effects on oocyte quality and maturation rates cannot be excluded, although dedicated seasonal control experiments were not performed. Because each RNA-seq replicate contained only 50 oocytes, the standard library preparation protocol may introduce

amplification bias and 3′/5′ coverage imbalance; the transcriptomic data should therefore be interpreted together with the qRT-PCR validation of VEGFA, FGF2, BCL-2 and BAX (Figure 6b–e).

5. Conclusions

Exogenous 50 ng/mL ghrelin accelerated bovine oocyte nuclear maturation through a multi-tiered cellular response, characterized by the upregulation of maturation-related genes, enrichment of PI3K–Akt- and GSH-related transcriptional signatures, and a more favorable redox/organelle fluorescence profile. Because phospho-Akt was not measured and LY294002 is not pathway-specific, the present data do not definitively establish PI3K–Akt signaling. Thus, the PI3K–Akt association should be regarded as a hypothesis-generating component of this hierarchical mechanism. Practically, these findings highlight the potential of ghrelin as a beneficial additive for IVM media to improve oocyte quality. Whether the accelerated maturation translates into improved developmental competence also remains to be determined by future IVF, embryo development, and transfer experiments.

Supplementary Materials: The following supporting information can be downloaded at: https://www.mdpi.com/article/10.3390/ani16233739/s1, Figure S1: Principal-component analysis (PCA) of transcriptome profiles from bovine oocytes under different ghrelin treatments and culture durations; Figure S2: GO enrichment bubble plot of differentially expressed genes between CON-16 h and G50-16 h bovine oocytes; Table S1: The primer sequences; Table S2: Summary of RNA-seq quality control metrics for all transcriptome libraries of bovine oocytes; Table S3: Bos_16h_G50vsBos_16h_con.GO enrich; Table S4: Bos_24h_convsBos_16h_G50.all_KEGG enrich; Table S5: Replicate-level first polar body extrusion rates and proportions of PB-extruded oocytes reaching MII stage in bovine oocytes across experimental groups.

Author Contributions: Conceptualization, R.J. and C.Z.; methodology, G.C. and Y.Z.; software, Z.L. and K.L.; validation, K.L. and X.F.; formal analysis, L.W.; investigation, Y.Y., D.W., Z.L. and X.Z.; resources, G.C.; data curation, X.F., X.Z. and L.W.; writing—original draft preparation, R.J.; writing—review and editing, C.Z.; visualization, D.W. and Y.Y.; supervision, Y.Z. and G.C.; project administration, C.Z.; funding acquisition, G.C. All authors have read and agreed to the published version of the manuscript.

Funding: This research was supported by the National Natural Science Foundation of China (No. 32260866) and the 2026 Research Support Fund—Construction of in-vitro Embryo Production Technical System for Cattle (No. RO2600000370).

Institutional Review Board Statement: All animal experiments were performed according to the regulations of the Administration of Affairs Concerning Experimental Animals in China. The experimental protocol was approved by the Animal Welfare and Research Ethics Committee of the Inner Mongolia Agricultural University (Approval ID: NND202608; approval date:21 August 2026). Ethical approval was obtained for all animal procedures performed in this study. This approval specifically covered the use of the Holstein donor cattle described in Section 2.2 and the ovum pick-up (OPU) procedures performed to collect oocytes from these animals for the present study.

Informed Consent Statement: Not applicable.

Data Availability Statement: The original contributions presented in this study are included in the article. The RNA-sequencing raw data have been deposited in the NCBI Sequence Read Archive (SRA) under BioProject accession number PRJNA1521568 (SRA submission number SUB16450497). The data will be publicly released upon publication of this manuscript. Further inquiries can be directed to the corresponding author.

Acknowledgments: The authors appreciate the efforts of every participant.

Conflicts of Interest: The authors declare no conflicts of interest.

References

1. Sirard, M.A.; Richard, F.; Blondin, P.; Robert, C. Contribution of the oocyte to embryo quality. *Theriogenology* **2006**, *65*, 126–136. [CrossRef]
2. Watson, A.J. Oocyte cytoplasmic maturation: A key mediator of oocyte and embryo developmental competence. *J. Anim. Sci.* **2007**, *85*, 1–3. [CrossRef]
3. Lonergan, P.; Fair, T. Maturation of oocytes in vitro. *Annu. Rev. Anim. Biosci.* **2015**, *4*, 3. [CrossRef]
4. Gilchrist, R.B.; Luciano, A.M.; Thompson, J.G. Oocyte-secreted factors: Regulators of cumulus cell function and oocyte quality. *Hum. Reprod. Update* **2008**, *14*, 159–167. [CrossRef]
5. Guérin, P.; El Mouatassim, S.; Ménézo, Y. Oxidative stress and protection against reactive oxygen species in the pre-implantation embryo and its surroundings. *Hum. Reprod. Update* **2001**, *7*, 175–189. [CrossRef]
6. Takahashi, M. Oxidative stress and redox regulation on in vitro development of mammalian embryos. *J. Reprod. Dev.* **2012**, *58*, 1–9. [CrossRef]
7. Combelles, C.M.; Gupta, S.; Agarwal, A. Could oxidative stress influence the in vitro maturation of oocytes? *Reprod. Biomed. Online* **2009**, *18*, 864–880. [CrossRef]
8. Koyama, K.; Kang, S.S.; Huang, W.; Yanagawa, Y.; Takahashi, Y.; Nagano, M. Aging-related changes in in vitro-matured bovine oocytes: Oxidative stress, mitochondrial activity and ATP content after nuclear maturation. *J. Reprod. Dev.* **2014**, *60*, 136–142. [CrossRef]
9. Ren, J.; Hao, Y.; Liu, Z.; Li, S.; Wang, C.; Wang, B.; Liu, Y.; Liu, G.; Dai, Y. Effect of exogenous glutathione supplementation on the in vitro developmental competence of ovine oocytes. *Theriogenology* **2021**, *173*, 144–155. [CrossRef]
10. Moran, B. Roles of mammalian glutathione peroxidase and thioredoxin reductase enzymes in the cellular response to nitrosative stress(Review). *Free Radic. Biol. Med.* **2018**, *127*, 160–164. [CrossRef]
11. Kojima, M.; Hosoda, H.; Date, Y.; Nakazato, M.; Matsuo, H.; Kangawa, K. Ghrelin is a growth-hormone-releasing acylated peptide from stomach. *Nature* **1999**, *402*, 656–660. [CrossRef]
12. Tena-Sempere, M. Ghrelin and reproduction: Ghrelin as a novel regulator of the gonadotropic axis. *Vitam. Horm.* **2008**, *77*, 285–300. [CrossRef]
13. Dupont, J.; Maillard, V.; Coyral-Castel, S.; Ramé, C.; Froment, P. Ghrelin in female and male reproduction. *Int. J. Pept.* **2010**, *2010*, 158102. [CrossRef]
14. Akalu, Y.; Molla, M.D.; Dessie, G.; Ayelign, B. Physiological effect of Ghrelin on body systems. *Int. J. Endocrinol.* **2020**, *2020*, 1385138. [CrossRef]
15. Kalous, J.; Aleshkina, D.; Anger, M. A role of PI3K/AKT signaling in oocyte maturation and early embryo development. *Cells* **2023**, *12*, 1830. [CrossRef]
16. Ferrer, B.; Suresh, H.; Tinkov, A.A.; Santamaria, A.; Rocha, J.B.; Skalny, A.V.; Bowman, A.B.; Aschner, M. Ghrelin attenuates methylmercury-induced oxidative stress in neuronal cells. *Mol. Neurobiol.* **2022**, *59*, 2098–2115. [CrossRef]
17. Li, X.Y.; Duan, J.X.; Wang, S.Y.; Cheng, J.Y.; Chen, H.L.; Zhang, Z.L.; Yang, L.; Hua, R.M.; Li, Q.W. Isorhamnetin protects porcine oocytes from zearalenone-induced reproductive toxicity through the PI3K/Akt signaling pathway. *J. Anim. Sci. Biotechnol.* **2023**, *14*, 1054–1067. [CrossRef]
18. Li, X.Y.; Cheng, J.Y.; Yao, Q.C.; Duan, J.X.; Chen, H.L.; Zhang, Z.L.; Yang, L.; Hua, R.M.; Li, Q.W. Isorhamnetin improves oocyte maturation by activating the PI3K/AKT signaling pathway. *Mol. Nutr. Food Res.* **2024**, *68*, e2300904. [CrossRef]
19. Li, K.W.; Zhao, G.P.; Zhang, Y.; Liu, Y. Effects of Ghrelin on in vitro maturation and in vitro fertilization of bovine oocytes. *Prog. Vet. Med.* **2025**, *46*, 64–69. (In Chinese) [CrossRef]
20. Love, M.I.; Huber, W.; Anders, S. Moderated estimation of fold change and dispersion for RNA-seq data with DESeq2. *Genome Biol.* **2014**, *15*, 550. [CrossRef]
21. Kim, D.; Langmead, B.; Salzberg, S.L. HISAT: A fast spliced aligner with low memory requirements. *Nat. Methods* **2015**, *12*, 357–360. [CrossRef]
22. Cossarizza, A.; Chang, H.D.; Radbruch, A.; Abrignani, S.; Addo, R.; Akdis, M.; Andrä, I.; Andreata, F.; Annunziato, F.; Arranz, E.; et al. Guidelines for the use of flow cytometry and cell sorting in immunological studies, third edition. *Eur. J. Immunol.* **2021**, *51*, 2708–3145. [CrossRef]
23. De Vos, M.; Grynberg, M.; Ho, T.M.; Yuan, Y.; Albertini, D.F.; Gilchrist, R.B. Perspectives on the development and future of oocyte IVM in clinical practice. *J. Assist. Reprod. Genet.* **2021**, *38*, 1265–1280. [CrossRef]
24. Sirini, M.A.; Anchordoquy, J.P.; Quintana, S.; Furnus, C.; Relling, A.E.; Anchordoquy, J.M. Expression of Ghrelin and its receptor mRNA in bovine oocyte and cumulus cells. *Int. J. Fertil. Steril.* **2019**, *12*, 335–338. [CrossRef]
25. Dashtizad, M.; Wahid, H.; Mazni, O.A.; Rosnina, Y.; Hajarian, H. Effects of Ghrelin on in vitro nuclear maturation and subsequent embryo development of immature bovine oocytes. *J. Anim. Vet. Adv.* **2011**, *10*, 2797–2801.
26. Thomas-Markos, C.; Chouzouris, E.; Dovolou, F.; Krania, I.S.; Pappas, K.; Dafopoulos, K. Effects of Ghrelin on activation of Akt1 and ERK1/2 pathways during in vitro maturation of bovine oocytes. *Zygote* **2017**, *25*, 183–189. [CrossRef]

27. Wang, D.; Yang, Y.; Song, Y.; Fu, S.; He, X.; Wang, B.; Wang, L.; Chen, X.; Li, X.; Liu, Y.; et al. The effect of Ghrelin on the maturation of sheep oocytes and early embryonic development in vitro. *Animals* **2022**, *12*, 1158–1169. [CrossRef]
28. Donadkar, M.; Kumar, B.; Singh, S.K.; Chandra, P.; Dangi, P.; Gawai, M.; Jackson, A.; Jasrotia, N.; Sharma, S.; Chouhan, V.; et al. Morpho-molecular evaluation for developmental competence of oocytes retrieved through transvaginal ovum pick-up from FSH-stimulated Tharparkar donor cows (*Bos indicus*). *Zygote* **2024**, *32*, 376–385. [CrossRef]
29. Wang, X.; Huang, F.; Li, X.; Hu, K.; Chen, H.; Niu, P.; Qu, H.; Fang, D.; Han, C.; Gao, Q. Transcriptomic analysis of bovine oocytes at GV and MII stages and dynamic changes in key gene expression patterns. *Biology* **2026**, *15*, 662. [CrossRef]
30. Han, S.J.; Vaccari, S.; Nedachi, T.; Andersen, C.B.; Kovacina, K.S.; Roth, R.A.; Conti, M. Protein kinase B/Akt phosphorylation of PDE3A and its role in mammalian oocyte maturation. *EMBO J.* **2006**, *25*, 5716–5725. [CrossRef]
31. Han, S.J.; Conti, M. New pathways from PKA to the Cdc2/cyclin B complex in oocytes: Wee1B as a potential PKA substrate. *Cell Cycle* **2006**, *5*, 227–231. [CrossRef]
32. Meanti, R.; Rizzi, L.; Bresciani, E.; Molteni, L.; Locatelli, V.; Coco, S.; Omeljaniuk, R.J.; Torsello, A. Hexarelin modulation of MAPK and PI3K/Akt pathways in Neuro-2a cells inhibits hydrogen peroxide-induced apoptotic toxicity. *Pharmaceuticals* **2021**, *14*, e14050444. [CrossRef]
33. Cory, S.; Adams, J.M. The Bcl2 family: Regulators of the cellular life-or-death switch. *Nat. Rev. Cancer* **2002**, *2*, 647–656. [CrossRef]
34. Gharbi, S.I.; Zvelebil, M.J.; Shuttleworth, S.J.; Hancox, T.; Saghir, N.; Timms, J.F.; Waterfield, M.D. Exploring the specificity of the PI3K family inhibitor LY294002. *Biochem. J.* **2007**, *404*, 15–21. [CrossRef]
35. Dua, D.; Alam, A.; Chauhan, M.S.; Palta, P.; Singh, M.K. Effect of vitrification on folliculogenesis-related genes in ovarian follicles of Bubalus bubalis. *Indian J. Anim. Res.* **2021**, *55*, 873–878. [CrossRef]
36. Du, C.; Davis, J.S.; Chen, C.; Li, Z.; Cao, Y.; Sun, H.; Shao, B.S.; Lin, Y.X.; Wang, Y.S.; Yang, L.G.; et al. FGF2/FGFR signaling promotes cumulus–oocyte complex maturation in vitro. *Reproduction* **2021**, *161*, 205–214. [CrossRef]
37. Zhou, Z.; Jia, R.X.; Zhang, G.; Wan, Y.; Zhang, Y.; Fan, Y.; Wang, Z.; Huang, P.; Wang, F. Using cysteine/cystine to overcome oxidative stress in goat oocytes and embryos cultured in vitro. *Mol. Med. Rep.* **2016**, *14*, 1219–1226. [CrossRef]
38. Kirillova, A.; Smitz, J.E.J.; Sukhikh, G.T.; Mazunin, I. The role of mitochondria in oocyte maturation. *Cells* **2021**, *10*, 2484. [CrossRef]
39. Settembre, C.; Fraldi, A.; Medina, D.L.; Ballabio, A. Signals from the lysosome: A control centre for cellular clearance and energy metabolism. *Nat. Rev. Mol. Cell Biol.* **2013**, *14*, 283–296. [CrossRef]

Disclaimer/Publisher's Note: The statements, opinions and data contained in all publications are solely those of the individual author(s) and contributor(s) and not of MDPI and/or the editor(s). MDPI and/or the editor(s) disclaim responsibility for any injury to people or property resulting from any ideas, methods, instructions or products referred to in the content.